Chapter 2

Dithienyl Ethene Switches and their Properties

The control of events at the molecular level is an important aspect in supramolecular chemistry. For effective application of molecular materials, facile synthetic routes that provide samples on sufficient large scale, along with easy structural modification, broad scope in addressability and non-destructive readout capabilities are required. In this chapter,[*] the major research theme which focusses on dithienylethene switches is introduced, as well as our contributions to understanding the basic physical properties of the perhydro- (and perfluoro) dithienyl molecular switches. Particular attention is placed on synthetic aspects (2.2) and addressability by photochemical (2.3) and electrochemical (2.4) means, along with the possible application of IR and Raman spectroscopy towards non-destructive read-out (2.5). The last paragraph (2.6) will give an overview on the other research interests and topics where this class of switches are being used.

* Part of this work was published: W.R. Browne, J.J.D. de Jong. T. Kudernac, M. Walko, L.N. Lucas, K. Uchida, J.H. van Esch, B.L. Feringa *Chem. Eur. J.* **2005**, 11, 6414-6429 & 6430-6441; D. Dulić, S.J. van der Molen, T. Kudernac, H.T. Jonkman, J.J.D. de Jong, T.N. Bowden, J. van Esch, B.L. Feringa, B.J. van Wees, *Phys. Rev. Lett*. **2003**, 91, *20*, Art. No. 207402; J.J.D. de Jong, L.N. Lucas, R.M. Kellogg, B.L. Feringa, J.H. van Esch, *Eur. J. Org. Chem.* **2003**, 10, 1887-1893; L.N. Lucas, J.J.D. de Jong, R.M. Kellogg, J.H. van Esch, B.L. Feringa, *Eur. J. Org. Chem.* **2003**, 1, 155-166; T. Kudernac. J.J. de Jong, J. van Esch, B.L. Feringa, D. Dulic, S.J. van der Molen, B.J. van Wees*, Mol. Cryst. Liq. Cryst*. **2005**, *430*, 205-210; P.R. Hania, A. Pugzlys, L.N. Lucas, J.J.D. de Jong, B.L. Feringa, J.H. van Esch, H.T. Jonkman, K. Duppen *J. Phys. Chem. A* **2005**, 109, 9437-9442. J.H. Hurenkamp, W.R. Browne, J.J.D. de Jong, L.N. Lucas, B.L. Feringa, J.H. van Esch, *manuscript in preparation*. J.J.D. de Jong, W.R. Browne, J.L. Barett, J.J. McGarvey, J.H. van Esch, B.L. Feringa, *manuscript in preparation*. M. Walko, J.J.D. de Jong, W.R. Browne, F. Hartl, J.J. McGarvey, J.H. van Esch, B.L. Feringa, *manuscript in preparation*.

2.1 Introduction in Molecular Switchable Systems

Although a large number of structurally diverse molecular switches are known,[1] they share common properties. Whereas the majority of small molecules exist in a single stable configuration, molecular switches are special in that they can exist in two geometries that are thermally stable (Figure 2.1). It is possible to change, or 'switch', between the two states by selective excitation of one state so that it transforms into the other.

Figure 2.1 *A molecular switch has at least two independently addressable stable states, which differ in a physical property, e.g. absorption, refractive indices, redox potentials, geometrical structure, etc. Reversibility, rapid response and thermal and fatigue stability are essential for their use in optoelectronic devices.*

Typically switching is achieved by light (optical switches) and / or redox changes (electrochemical switches), however, in principle any non-destructive trigger can be employed to induce a reversible change in the system. Furthermore, it should be possible to 'read' the state of the molecule, without destroying the information contained by the molecule, i.e, non-destructive read-out. There are several key features that the responsive part should have. It should be selectively addressable, fatigue resistant, and be capable of non-destructive readout. The toolbox for synthetic organic chemists in the field of photochromic switches is centered around five different molecular switching units, with the structures of the four not studied in this thesis depicted in Figures 2.2-2.5. All four switches have different properties, which can be exploited.

Azobenzene compounds (Figure 2.2) were among the first molecular switches used and are still the subject of extensive investigation.[2] There is a large spatial difference between cis and trans forms, while photoconversion yields are generally high. Major difficulties are the relatively minor changes in the absorption spectra upon isomerisation and the often low thermally stability of the cis form.

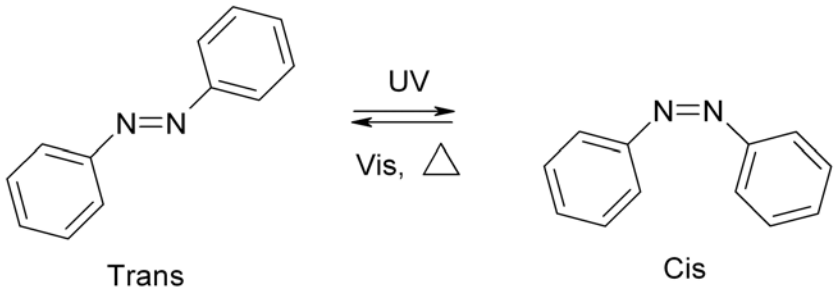

Figure 2.2 *Azobenzene compounds, which isomerize upon irradiation with UV light from a stable trans to a thermally unstable cis configuration. Upon irradiation with visible light (or less favorably thermally) the reverse reaction occurs.*

Overcrowded alkenes[3] (Figure 2.3) can have an intrinsically chiral structure and the interconversion between either *P* or *M* helicity by photoisomerisation around a central double bond allows for its use as chiroptical switches. This makes them excellent candidates for detection and observation by circular dichroism (CD) spectroscopy. Changing substituents (Z_1 and Z_2) on the lower half to a nitro-arene acceptor and a dimethylamino-arene donor moiety allows for tuning of the system, leading to higher photoconversions and larger differences in the absorption spectra.[4] These compounds were the basis for the first light-driven unidirectional molecular motor.[5]

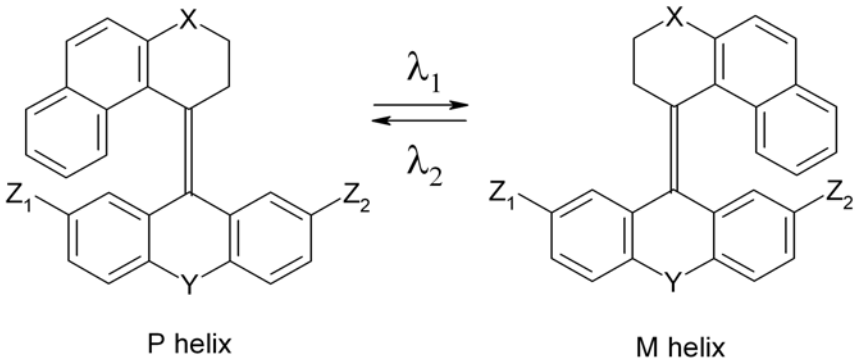

Figure 2.3 *Overcrowded alkene, which changes between a P and M helix upon irradiation. The central double bond is enlongated for clarity only.*

Spiropyrans[6] (Figure 2.4) are an interesting class of molecular switches since the open form exist as a stable zwitterion (merocyanine). Upon irradiation with visible light the colored merocyanine undergoes a 6π electron ring closure to the colorless spiropyran and the reverse reaction can be accomplished with UV light. This unique feature can be exploited for specific interactions within local environments, due to the strong change in dipole and in the hydrophobicity.

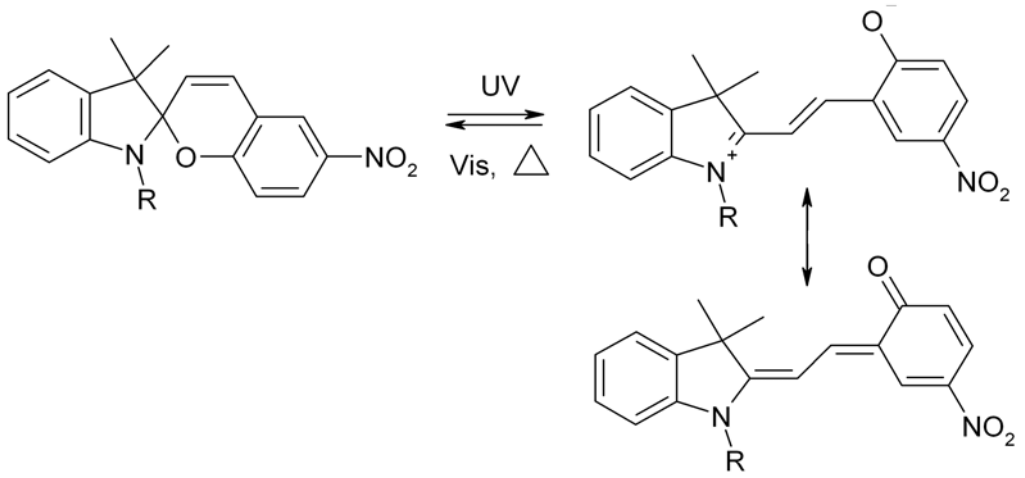

Figure 2.4 *Spiropyran which changes between a neutral and zwitterionic species (merocyanine form) upon irradiation with either UV or visible light.*

An other interesting class of photochromic switches, the fulgides, are known already for a century.[7] They can exist in three different configurations as depicted in Figure 2.5; the Z form, the E form, which are colorless geometrical isomers, and the C form which is highly colored. The E and C form can photoisomerize into one and other upon irradiation with UV light (E → C) or visible light (C → E), whereas the Z form is an unwanted isomerisation. In this Z form the aromatic moiety is on the wrong side to undergo a 6π electron ring closure to the C from, lowerin the overall photochemical efficiency. In 1981 a breakthrough in fulgide photochemistry was achieved[8] when the first thermally irreversible fulgide was synthesized, and since then they have been used in a wide range of applications. They resemble closely the fifth family of switches, the diarylethenes.

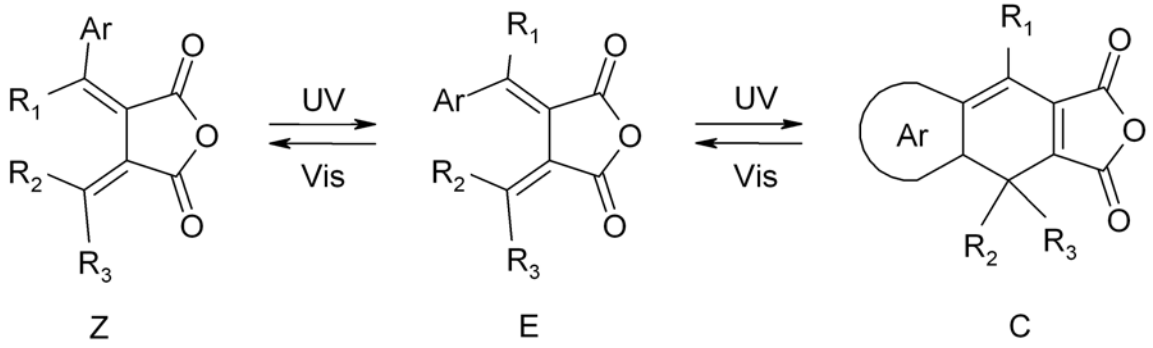

Figure 2.5 *Fulgide switch where three states can be addressed by light; C, E and Z structures.*

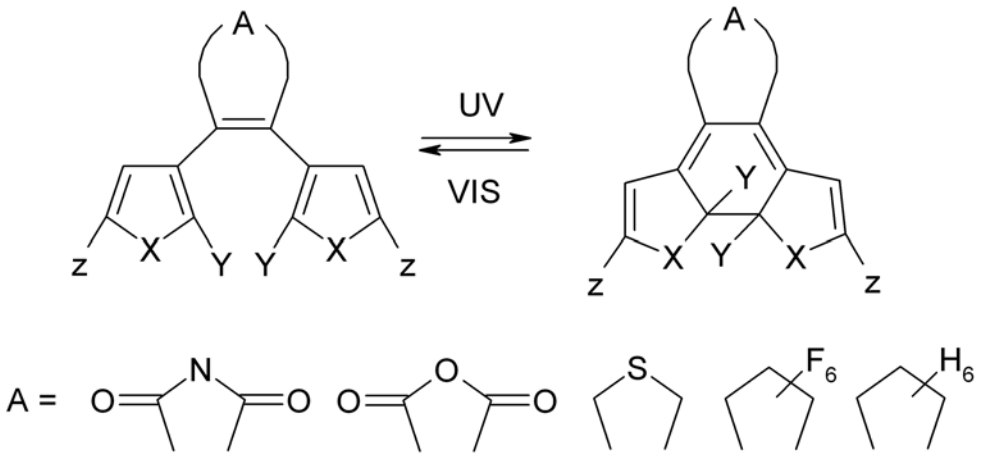

Figure 2.6 *General structure for diarylethenes. Several bridging units have been employed (A), along with a wide variety of aromatic groups (X) and side groups (Y and Z). In this chapter either perhydro or perfluoro cyclopentenes (A) as bridging units are discussed in combination with thiophene units (X = S).*

The fifth class of molecular switch comprises the diaryl ethenes,[9] which are most commonly used primarily due to their good photophysical properties (Figure 2.6). The central core consists of a triene (6π electrons) that can undergo cyclization upon irradiation with UV light in a conrotatory fashion to a ring closed form (Figure 2.7). The thermal back reaction is symmetry forbidden giving them good thermal stability. Furthermore they combine high fatigue resistance, up to 10^4 cycles for some systems have been reported, with good quantum yield and facile synthesis. There have been two recent reviews[10] which reflects the current interests in diarylethenes and give a summary of the most important features of these important photoactive materials. In the following sections the most important properties of dithienyl switches will be highlighted. First the synthetic availability of dithienyl ethenes will be discussed briefly (2.2). Then the addressability using photochemical (2.3) and the recently developed electrochemical switching (2.4) will be mentioned. This is followed by recent results with detection (read-out) using IR and Raman spectroscopy (2.5). Finally, some other applications will be described, including incorporation into polymers, molecular switchable devices, fluorescence properties and photochemical aspects in the crystalline state (2.6).

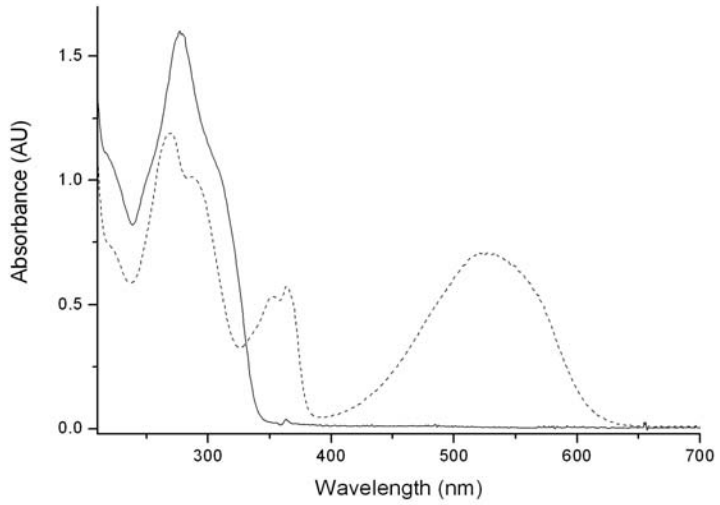

Figure 2.7 *Representative UV/Vis spectrum of* ***1H*** *the colorless open form (dark line) and the colored closed form (dotted line).*

2.2 Synthesis of Dithienyl Cyclopethene Switches

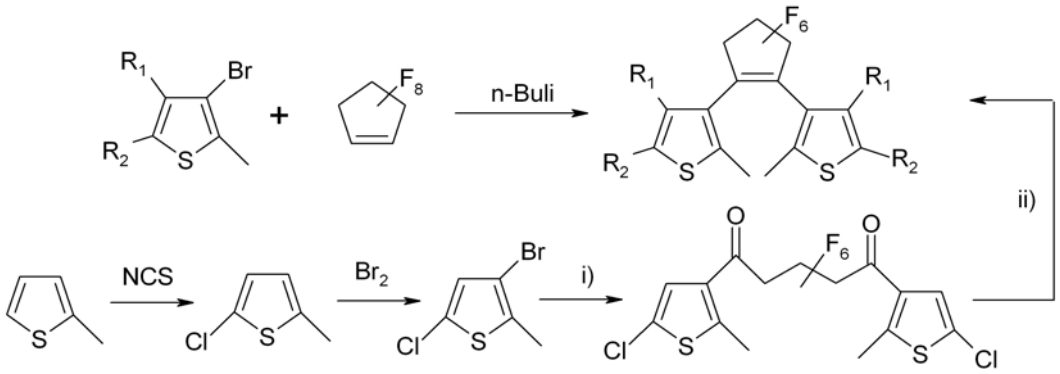

Figure 2.8 *Synthesis of perfluoro dithienyl switches (**F**). Top; original synthesis using octafluorocyclopentene and a lithiated thiophene. Bottom; alternative synthesis, starting from methylthiophene followed by halogenenation at the 5-position. Subsequent 1,2-addition to a diester and McMurry coupling resulted in the versatile dichloro-substituted switch. i) n-Buli, hexafluoroglutaryl ethyl ester. ii) Zn, $TiCl_4$, THF (R_1 = H and R_2 = Cl).*

Previously, synthetic routes to perfluoro dithienylethenes required the use of octafluorocyclopentene, which boils at 28 °C, is difficult to handle, and is very expensive. In a general synthesis procedure, the desired bromo substituted thiophene would be lithiated at -78 °C and subsequent nucleophilic addition to the fluorinated alkene resulted in the desired switch by addition elimination reactions (Figure 2.8).

Recently, a more ecomomic and more versatile procedure was developed in our laboratories based on an intramolecular McMurry coupling as a key step (Figure 2.8).[11,12,13] In addition to lower cost, the synthetically flexible chloride group attached to the R_2 position allows for facile functionalization.

Although the perfluoro switches have better switching properties, *i.e*. higher fatigue resistance and improved thermal stability, the corresponding perhydro switches (Figure 2.9) are excellent building blocks to incorporate as switchable units in molecular systems that function as smart materials,[14] due to lower synthetic costs. Halogenation of methylthiophene occurs selective at the 5-position. Subsequent Friedel-Crafts acylation with glutaryl chloride is exclusive on the 4-position, to give a black tar. This material can be reacted without purification in a McMurry coupling using Zn powder and $TiCl_4$ in THF. Again a black tar is obtained, which can be flushed over a silica column using pentane as an eluent to obtain **7H** as a white crystalline material in 25-40% overall yield in three steps. Reactions have been performed on large scale yielding up to 25 g of **7H**.

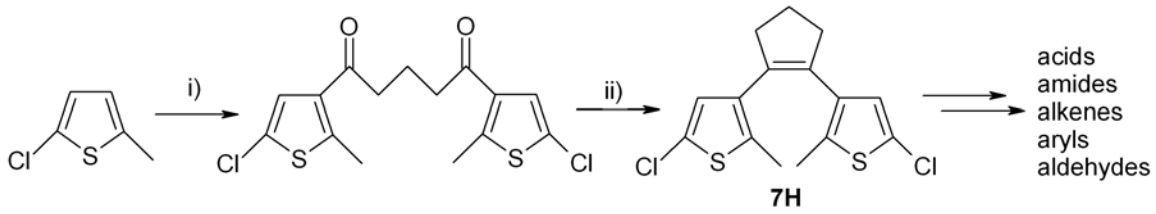

Figure 2.9 *Synthesis for perhydro switch (**H**). i) glutaryl chloride, $AlCl_3$, CS_2 or nitromethane ii) Zn, $TiCl_4$, THF to yield **7H** in 25-40% yield (3 steps). The chlorine moiety can be transformed to a wide variety of functionalities including acids, amides, imines, alkenes and aryls (see Figure 2.10 for derivatives).*

The chloride group can be used in palladium cross coupling employing the Suzuki reaction to introduce aromatic units such as thiophenes, pyridines and substituted benzenes. Alternatively, lithiation and subsequent reaction with an electrophile introduces a carboxylic acid group (for further reaction to amides, see Chapter 3) or aldehyde group, which can be transformed into imines or alkenes. With this synthetically versatile 'toolbox' of functionalized diaryl ethenes, a wide library of derivatives can be prepared. However, only a few representative switches were prepared to explore the properties discussed in the following paragraphs (Figure 2.10). Several substituted benzenes (**1H-6H**, **18H**, **19H**), thiophenes (**11H**, **12H**, **14H-17H**) and pyridines (**13H-15H**) were introduced via Suzuki coupling, with either electron withdrawing (**3H**) or donating moieties (**2H**, **4H**, **5H**). Also extension of side groups with additional aromatic units in series (**14H-18H**) and the related aldehyde (**9H**) and ester (**10H**) derivatives were

prepared. For comparison, several analogous substituted hexafluoro switches were also synthesized (**1F-3F**, **7F**, **9F**).

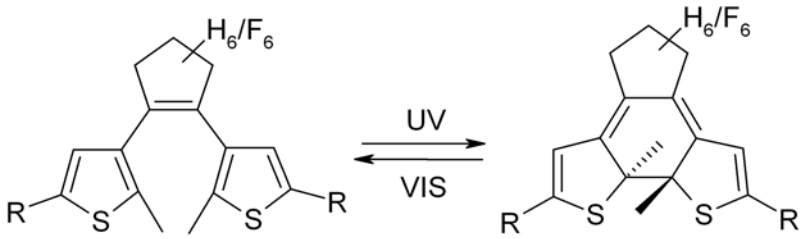

Ho / Fo **Hc / Fc**

1H R = Ph	**7H** R = Cl	**13H** R = Py	**19H** R = PhBr-m
2H R = PhOMe	**8H** R = Me	**14H** R = ThPy	**1F** R = Ph
3H R = PhCN	**9H** R = CHO	**15H** R = ThThPy	**2F** R = PHOMe
4H R = PHSMe	**10H** R = CO_2Et	**16H** R = ThTh	**3F** R = PhCN
5H R = PhSAc	**11H** R = Th	**17H** R = ThPh	**7F** R = Cl
6H R = PhBr	**12H** R = ThSAc	**18H** R = $PhPhOC_6H_{13}$	**9F** R = CHO

Figure 2.10 *Substituted diaryl ethenes synthesized and studied in this chapter.*

2.3 Photophysical Properties

Dithienylethene switches exist in two different states, namely the open (**Fo** and **Ho**) and closed form (**Fc** and **Hc**). Upon irradiation the open form tranforms by a 6-π electron cyclisation into the closed from.[15] In the open form, there is little electronic interaction over the central double bond, because of the nonplanar structure, e.g. no conjugation the between the two thiophene halfs across the central double bond. However, ring closure to the closed form leads to considerable electronic interaction between the two thiophene moieties due to the formation of a conjugated planar system. Hence the open form is colorless and the closed form is colored, ranging from yellow, red, purple to blue depending on the R substituents. The standard technique to observe switching is by UV/Vis detection. A detailed list of the electronic absoption data in acetonitrile solution is presented in Table 2.1.

For the open form, the UV absorption spectra of **1-6Ho** shown in Figure 2.11a are representative for this class of compounds (see also Table 2.1). The effect of incorporating a hexahydro cyclopentene group instead of a hexafluoro cyclopentene group on the absorption spectra of the dithienylethenes (*e.g.*, **1Ho** - λ_{max} = 278 nm and **1Fo** - λ_{max} = 285) is quite modest, especially, considering the very large difference in the redox properties (Chapter 2.4) of the hexahydrocyclopentene (**1H-11Ho)** and

hexafluorocyclopentene (**1F-3F, 7F, 9Fo**) based compounds (Figure 2.10). In contrast, the effect of substitution in the C5 position of thiophene ring is much more pronounced with the λ_{max} changing by up to 50 nm (~ 5000 cm^{-1}) in this series.

Table 2.1 Electronic and photochemical properties of open and closed forms in CH_3CN.

	Substituents	PSS	Open form λ_{max} / nm (ε /10^3 cm^{-1} M^{-1})	Closed form λ_{max} / nm (ε /10^3 cm^{-1} M^{-1})	
1H	R = Ph	0.99	278 (18), 303 (S)	267 (15), 287 (S), 331 (I, 13), 349 (5.2), 360 (6.4)	527 (8.8)
1F	R = Ph	0.92	285 (33)	307 (I, 22), 308 (22), 366 (8.8), 380 (9.1)	588 (12)
2H	R = PhOMe	0.99	284 (28), 308 (S)	237 (14), 273 (S), 303 (24), 329 (12), 345 (9.5), 348 (S)	519 (13)
2F	R = PhOMe	0.99	296 (38)	321 (I, 21), 344 (25), 376 (S)	593 (18)
3H	R = PhCN	0.99	229 (31), 300 (35)	287 (36), 366 (I, 11), 387 (14)	575 (22)
3F	R = PhCN	0.99	232 (17), 315 (9.0)	341 (I, 9.4), 374 (5.6), 395 (S)	586 (5.9)
4H	R = PhSMe	0.96	295 (S), 320 (35)	344(I, 19), 364 (S)	540 (18)
5H	R = PhSAc	[3]	295 (49), 322 (49)	345 (I), 364 (S)	541
6H	R = PhBr	0.99	282 (47), 313 (S)	340 (I, 17), 355 (18), 366 (18)	532 (24)
7H	R = Cl	[1]	236 (19)		444
7F	R = Cl	0.45	242 (22), 305 (4.1)	264 (I, 3.9), 287 (I, 2.0), 305 (I, 2.0), 326 (2.7), 338 (S)	504 (2.1)
8H	R = Me	[1]	234 (22), 273 (S)		[2]
9H	R = CHO	0.95	269 (25), 315 (8.2)	218 (I, 11), 236 (I, 12), 336 (I, 5.7), 372 (9.3)	577 (8.2)
9F	R = CHO	0.95	263 (29), 294 (18)	239 (I, 11), 320 (I, 4.5), 344 (5.1), 395 (6.0)	614 (6.4)
10H	R = CO_2Et	0.78	258 (27), 297 (S)	316 (I, 21), 354 (21)	540 (21)
11H	R = thienyl	0.98	281 (14), 295 (18)	229 (10), 311 (18), 347 (8.5), 356 (9.5), 369 (S)	519 (13)

PSS (maximum % of closed state formed by photolysis at λ = 313 nm) in CH_3CN, I = isosbestic point, S = shoulder [1] PSS not determined due to overlap of the signals for the open and closed form in the ^1H NMR spectrumy. [2] not determined, no clear signal changes occur during irradiation with 313 nm. [3] very low solubility in CH_3CN precluded accurate measurement by ^1H NMR spectroscopy.

In the closed form (*e.g.,* **1-6Hc**, Figure 2.11b), the effect of substitution at the C5 position of the thienyl ring is similar to that observed in the open state. The molar absorptivity shows a marked increase accompanied by a bathochromic (red) shift with increasing electron donating character of the substituent in the *para*-position of the phenyl ring (Table 2.1).[16] The changes observed in the near UV region of the spectrum (250-400 nm) upon substitution are considerable, with the changes in the band at ~ 360 nm similar to those of the ~ 550 nm band. The absorptions in the UV region show a different substituent dependence to the visible absorption bands. For the non-aryl substituted compounds (*e.g.,* **7-10H/F**) only the chloro-substituted compound (**7H/F**) displays markedly different (hypsochromically shifted) spectroscopic properties compared to the aryl-substituted compounds.

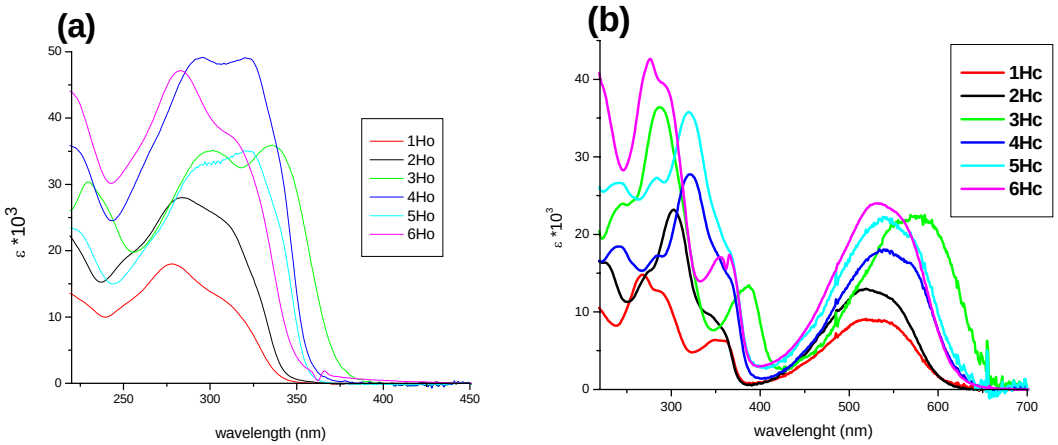

Figure 2.11 *UV/Vis absorption spectra of (a)* ***1Ho-6Ho****, and (b):* ***1Hc-6Hc*** *in acetonitrile at room temperature (typical concentrations are* 10^{-5} *M)***.**

For C5-substituted derivatives a bathochromic (red) shift of 60 nm (2200 cm^{-1} +/- 250 cm^{-1}) is observed upon substitution of the hexahydrocyclopentene unit with the hexafluorocyclopentene unit (*e.g.,* **1Hc** to **1Fc**, **3Hc** to **3Fc** etc.). For the majority of C5-substituted compounds the effect of substitution, *i.e.,* the shift in the lowest absorption band compared with **1Hc** or **1Fc**, is similar. The benzonitrile-substituted hexafluoro-compound **3F** shows only a very modest bathochromic (red) shift compared with **3Hc**, indicating that the electron withdrawing properties of the perfluoro bridge are conflicting with the electron withdrawing capability of the nitrile.

Ring opening (*e.g.,* **1Hc** to **1Ho**) and ring closure (*e.g.,* **1Ho** to **1Hc**) of these compounds in acetonitrile (by irradiation at $\lambda > 460$ nm and at $\lambda = 313$ nm, respectively) was monitored by UV/Vis spectroscopy. Since there is significant overlap for both the open and closed form in the UV region it is not possible to selectively excite the open form since both will be absorbing light. Therefore a photo-stationary state (PSS) is expected, which is the equilibrium of both open and closed form while being irradiated at that specific wavelength. This equilibrium depends on the quantum yield of both conversions and the extinction coefficients of both the open and closed forms of the molecules. Since the open form does not absorb in the visible, the closed from can be selectively excited and complete conversion of the closed to the open form is possible.

The PSS was determined by ^{1}H NMR spectroscopy for these compounds (Table 2.1). Upon irradiation at $\lambda = 313$ nm, absorption bands in the visible region appeared (300 to 700 nm) and with subsequent irradiation of the closed form (at $\lambda > 460$ nm) complete

recovery of the open form is observed. This process could be repeated at least 3 times with minimal degradation (< 5 %). It should be noted, however, that a solvent-dependence on the extent of degradation was observed with solvent purity being an important factor. This suggests that the degradation observed may not, for the major part, be inherent to the dithienylethene systems. With the exception of **5H**, **7H/F,** and **10H**, all compounds show a PSS with 90 and 99 % of the closed form upon irradiation (λ = 313 nm) as determined by ^{1}H NMR, despite the non-zero overlap in the absorption of the open and closed form. The high PSS states achieved indicate that as with toluene, in acetonitrile the quantum yields for photochemical ring opening are considerably lower than those of ring closure, since the extinction coefficients are roughly similar. For **7F**, the very low PSS is most likely due to the low absorption of **7Fo** and the relatively high absorption of **7Fc** at the wavelength employed for ring closure (λ= 313 nm).

2.4 Electrochemical Properties

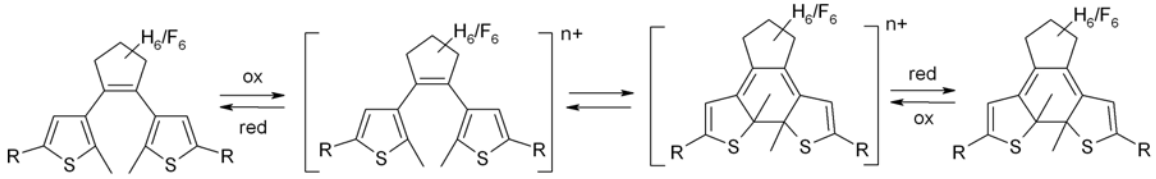

Figure 2.12 *Simplified process for electrochemical switching of* ***H*** *and* ***F****. Upon oxidation the neutral switch becomes positively charged, which results in either ring closing (for* ***H****) or ring opening (for* ***F****). See text for details.*

Typically only UV and visible light are used to address (or trigger) these switches as described in the previous section, however, reports on γ-irradiation[17] and electrochemical switching[18] have appeared. The use of redox-active groups covalently attached to the dithienylethenes has been examined in an effort to marry the electronic and redox properties in multicomponent systems,[19,20] however, until very recently, have the electrochemical properties been explored only in a few samples. The redox chemistry of dithienylethenes received some attention in recent reports on electrochemical ring opening and closing.[21] The electrochemical properties of hexahydro- and hexafluoro-dithienylcyclopentenes of the oxidized compounds in the +1 and +2 oxidation state are summarized in Table 2.2. The possibility of electrochemical cyclisation (Figure 2.12) and cycloreversion was explored through UV/Vis spectroelectrochemistry. The effect of electrolyte, solvent and temperature on the spectroelectrochemical properties were examined, and the switching process was found to be very sensitive to the donor

properties of the solvent / electrolyte system employed. In addition a thermally activated reversible isomerisation of the dicationic-closed form was observed.

Table 2.2 Redox properties of (dithienyl) cyclopentenes

		Open form (V vs SCE)		**Closed form $E_{½}$ (V vs SCE)**		**ΔE (mV)**
		$E_{p,a}$	**$E_{p,c}$**	**($E_{p,a}$ where *irr*)**	**($E_{p,c}$ where *irr*)**	
1H	R = Ph	1.16 (*irr*)	-2.53 (*irr*)	0.67, 0.43	-1.74, -2.03	240
1F	R = Ph	1.59 (*irr*)	-1.75 (*irr*)	0.85 (*qr*)	-1.13 (*qr*)	
2H	R = PhOMe	0.99 (*irr*)		0.45, 0.32	-1.84 (*irr*),-2.16 (*irr*)	130
2F	R = PhOMe	1.20 (*irr*)	-1.70 (*irr*)	0.67	-1.16 (*irr*),-1.46 (*irr*)	
3H	R = PhCN	1.29 (*irr*)	-2.06 (*irr*)	0.78, 0.53	-1.4 (*irr*)	250
3F	R = PhCN	1.46 (*irr*)		1.05 (*irr*)	-0.83 (*irr*)	
4H	R = PhSMe	0.89 (*irr*)		0.44, 0.30		140
5H	R = PhSAc	0.97 (*irr*)		0.50, 0.35	-1.70 (*irr*)	150
6H	R = PhBr	1.15 (*irr*)		0.69, 0.47		220
7H	R = Cl	1.37 (*irr*)		0.815 (*irr*), 0.63		125
7F	R = Cl	2.03 (*irr*)	-1.70 (*irr*)	1.15 (*irr*)	-1.10 (*irr*)	
8H	R = Me	1.105 (*irr*)		0.47, 0.37		100
9H	R = CHO	1.46 (*irr*)		1.13 (*irr*), 0.86 (*qr*)		240
9F	R = CHO	2.25 (*irr*)	-1.50 (*irr*)	1.35 (*irr*)	-0.42 (*irr*)	
10H	R = CO_2Et	1.53 *(irr),* 1.43 (*irr*)		1.12 (*irr*), 0.81	-1.22, -1.36	280
11H	R = thienyl	1.06 (*irr*)		0.53, 0.40	-2.28 (*qr*)	130

*Concentrations **1H-11H** and **1F-2F**, **7F**, **9F** are between 0.3-1.1 mM in 0.1 M TBAP/CH_3CN. irr = irreversible,[22] qr = quasireversible,[22] ΔE = separation between the 1st and 2nd oxidation processes of the closed form. Note that $E_{½}$ is given when not (irr).*

The effect of variation in the central cyclopentene moieties (perfluoro vs. perhydro) on the redox properties (Table 2.2) is quite large in contrast to the effect on their photochemical properties (Table 2.1). As has been reported previously for related compounds,[19,20,21] in the open state all of the compounds examined exhibit an irreversible oxidation process at more anodic potentials than in the closed state. The hexahydro- and hexafluorocyclopentene units represent extreme limits in terms of the electronic properties of the bridging cyclopentene unit and hence significant differences in the redox properties of the two sets of dithienylethene compounds are observed. For the phenyl substituted compounds (**1H/1F**) very large anodic shifts in the both oxidation (Δ 420-430 mV) and reduction (Δ 670-780 mV) processes are observed, indicating that the hexafluoro substitution serves to stabilise the LUMO (*i.e.,* the first reduction process) to a greater extent than the HOMO (*i.e.,* the first oxidation process).

For the aryl-substituted compounds (**2H-6H**) a correlation between the inductive effect of the substituent (σ_I)[23] and the redox properties of the open and closed forms was observed. However, the lack of any correlation with resonance parameters suggest that delocalisation of the HOMO over the aryl ring is not an important feature of these systems. Interestingly the trend holds both for the neutral compounds and for the mono-cations, which suggests that even in the oxidised state delocalisation of the SOMO over the phenyl rings is not significant.[24] All redox processes undergo an anodic shift (210-790 mV) upon substitution of the hexahydro- for the hexafluoro-cyclopentene unit in accordance with the electron withdrawing character of the perfluoro substituted cyclopentene unit, however the shift is less for the first oxidation process than for the first reduction process. The anodic shift observed for the open forms is similar to that observed for the first oxidation process in the closed forms, with the exception of **2Ho**/**2Fo** and **3Ho**/**3Fo**. The reduced anodic shift observed for these compounds is due to the non-innocent nature of the substituted aryl groups of the hexafluoro compounds in the open form. For **3Hc**/**3Fc** the anodic shift is comparable for both the first reduction (530 mV) and first oxidation processes (520 mV), which implies a modest (400 cm^{-1}) red shift between **3Hc** and **3Fc**.

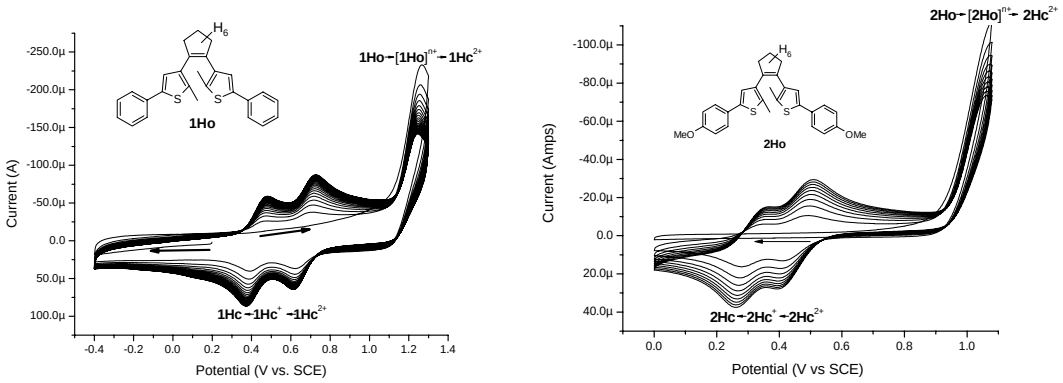

Figure 2.13 *Oxidative conversion of **1Ho** to **1Hc** by (50 cycles) left, and **2Ho** to **2Hc** right, by repetitive cyclic voltammetry at 0.5 Vs^{-1} in 0.1 M TBAP/CH_3CN. Initial scan direction is cathodic and starting point is 0 V vs SCE.*

Typical cyclic voltamograms are shown in Figure 2.13 for **1Ho** and **2Ho** which result in ring closure upon oxidation to **1Hc** and **2Hc** (*vide infra*)**.** In the open state a cathodic shift (150 mV) is observed upon introduction of a methoxy substituent, reflecting the electron donating properties of this group. In contrast to the closed forms, the open form shows a single irreversible two-electron[25] redox process at anodic potentials, typical of thiophene oxidation chemistry.[26] For both **1Ho** and **2Ho** oxidation is completely irreversible.

Indeed with a Pt (10 μm) microelectrode, no reversibility in the oxidation of the open form **1Ho** was observed at scan rates up to 1000 V s^{-1} placing the rate for the ring closure reaction at > 10^4 s^{-1}. However, on the return cycle two new reduction processes are observed at potentials coincident with those of the closed forms, e.g. electrochemical ring closure occurs! Repetitive cycling at high scan rates results in a significant build up of the closed form (from **1Ho** to **1Hc** and **2Ho** to **2Hc**) within the diffusion layer of the electrode (Figure 2.13).[27,21] For **1Hc** and **2Hc** two fully reversible oxidation processes are observed between 0.0 and 1.0 V (vs. SCE), assigned to two one electron oxidation steps, in agreement with the data obtained by starting from **1Ho** and **2Ho**. Thus for perhydrocylopentene diarylethenes electrochemical ring closure occurs readilly upon oxidation.

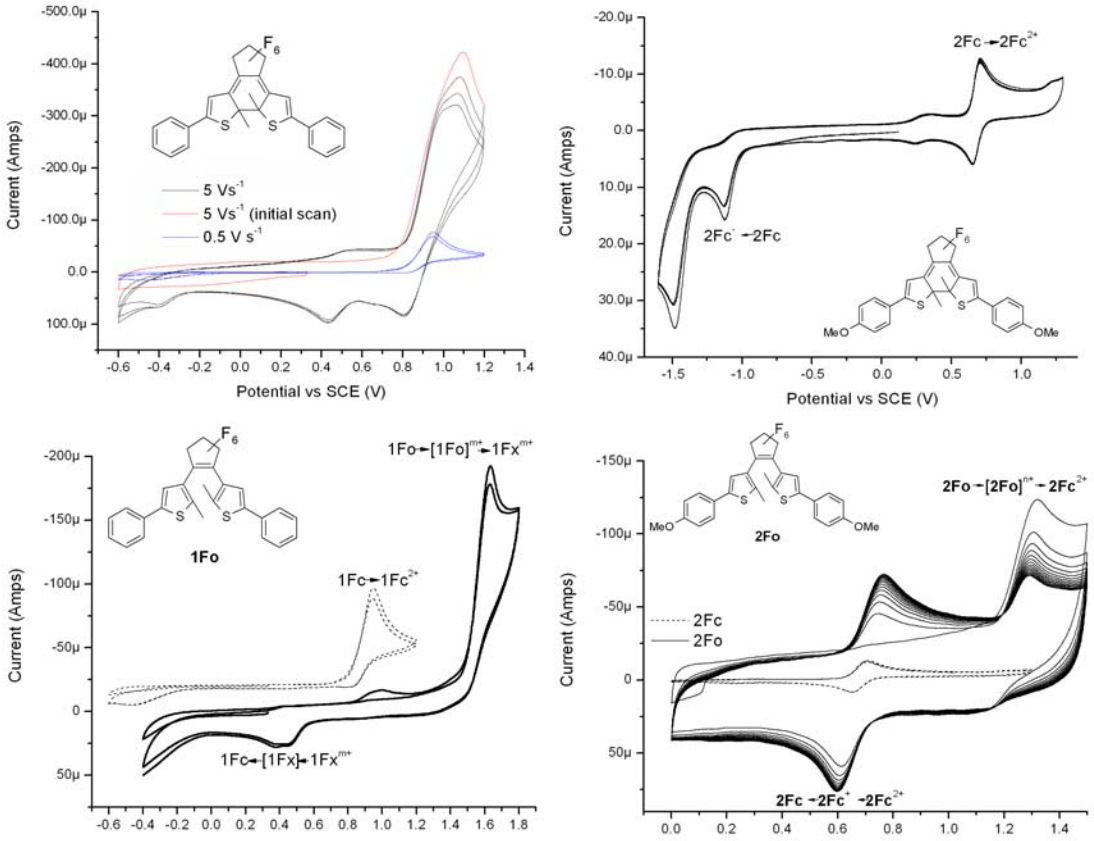

Figure 14 *top: Cyclic voltammetry of* ***1Fc*** *(left) at 0.5 and 5 Vs^{-1} and* ***2Fc*** *at 0.1 V s^{-1} (right) in CH_3CN (0.1 M TBAP). Bottom: Cyclic voltammetry of* ***1Fc/1Fo*** *(left) and,* ***2Fc/2Fo*** *(right) at 0.5 Vs^{-1} (0.01 M TBAP in CH_3CN). Initial scan direction is cathodic and start point is 0 V vs SCE. See text for details.*

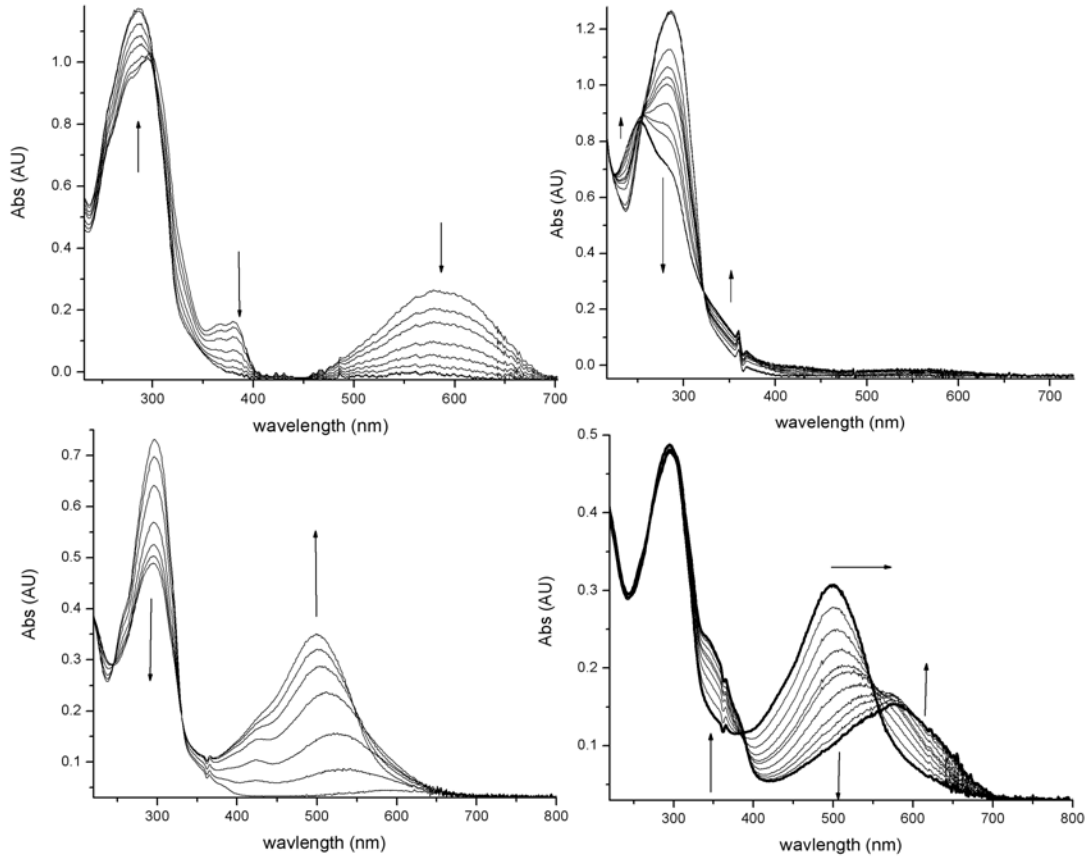

Figure 2.15 *Top: oxidation of* ***1Fc*** *(left) at 1.0 V to* ***1Fo*** *and oxidative degradation of* ***1Fo*** *(right) at 1.4 V at 273 K in 0.1 M TBAP/CH_3CN. Bottom: oxidation of* ***2Fo*** *at 1.4 V (left) followed by reduction of the oxidation product at 0 V to* ***2Fc*** *(right).*

For all other derivatives tested, except **7H** and **8H**, similar behavior was observed (Table 2.2); upon oxidation of the perhydrocyclopentene switch electrochemical ring closure occurs, which results in the closed form after reduction of the charged intermediate. Electrochemistry combined with UV/Vis spectroscopy is a powerful way to observe *in situ* the changes upon oxidation and reduction, which is shown for **1F** and **2F** in Figures 2.14 and 2.15. Oxidation of **1Fo** at 1.4V leads to degradation as observed by the loss in absorbance of the switch, whereas for **1Fc** a *quasi*-reversible oxidation is observed at 0.85 V and a quasi-reversible reduction at –1.13 V. At high scan rates (> 2 Vs^{-1}), two oxidation processes for **1Fc** are partially resolved (30 mV < ΔE < 50 mV) and two reduction waves are observed on the return cycle. The scan rate dependence of the reversibility suggests that the oxidation processes are electrochemically reversible and that the irreversibility observed at low scan rates is due to a moderately slow (10^{-3} to 10^{-2} s^{-1}) subsequent chemical reaction (an EC mechanism).[28] For **2Fc** the reversibility of the

oxidation is considerably improved and two quasi-reversible reductions were also observed indicating that a more complex electrochemical behaviour is present than for **1Fc**. The reduction in ΔE from **1Fc** to **2Fc** is in agreement with that observed for **1Hc** to **2Hc**. For both **2Hc** and **2Fc**, however, the similarity of the redox properties and potentials with those of the phenyl substituted compounds **1Hc** and **1Fc**, provide strong evidence that the electrochemical processes observed are based on the dithienylethene core and not on the methoxyphenyl substituents. For **2Fo** an irreversible oxidation process at 1.2 V is observed, however, in contrast to **1Fo**, for **2Fo** ring closure is found upon oxidation of the open state (Figure 2.15). This remarkable difference in electrochemical behaviour between **1Fo** and **2Fo**, together with the large difference in oxidation potential (400 mV) suggests that in contrast to **2Ho**, for **2Fo** the oxidation process involves the methoxyphenyl unit and not the dithienylethene unit.

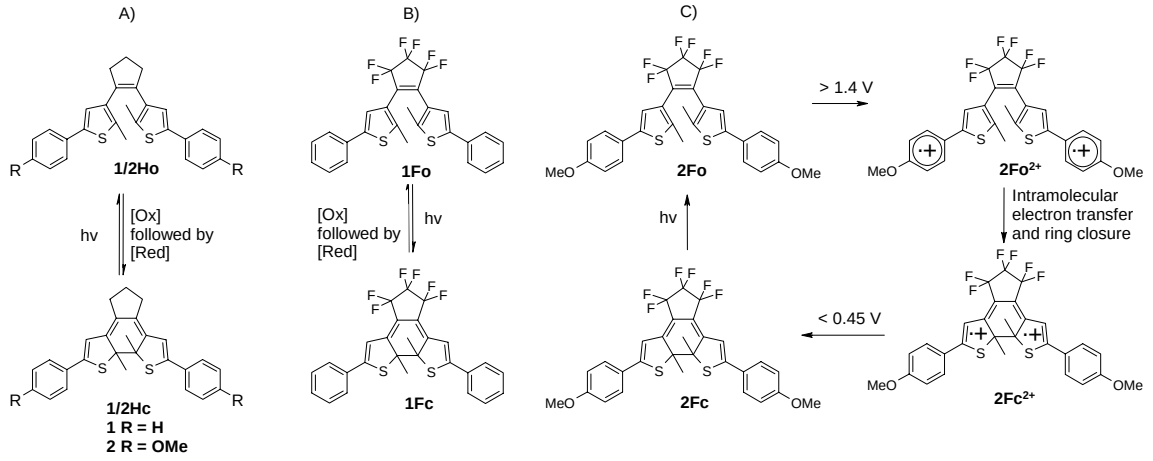

Figure 2.16 *Tuning of direction of electro- and photo-chemical ring opening/closing. A) For **1H/2H** oxidative (followed by reduction) ring closure takes place whereas for B), **1F**, oxidative (followed by reduction) ring opening is observed. C) the proposed mechanism for ring closure during the oxidation of **2Fo**.*

The results for the experiments are summarized in Figure 2.16.[29] The CV experiments combined with UV/Vis spectroscopy clearly show that for **1H/2H** electrochemical ring closure is observed (Figure 2.13) whereas for **1F** electrochemical ring opening is seen. This can be changed by introducing non-innocent side groups as for **2F**, which invert the electrochemical switching (Figure 2.14-2.15). This 'tunability' in the direction of the reaction can be explained by understanding the underlying driving force for ring opening and closing. Assuming that the two thienyl rings of the open form (and by analogy the two trans-butadiene systems of the closed form) behave as independent redox units then it is possible that the most important factor is the relative stabilisation of the cation based

on the thiophene heterocycle (*i.e.*, in the open form) compared with the cation based on the extended trans-butadiene (*i.e.*, in the closed form). To a first approximation the hetero cyclic cation would be expected to be the most stable state and hence the natural direction of electrochemical switching is from the closed to the open form. However, in the hexahydrocyclopentene based compounds, the positive charge of the cation is sufficiently delocalised over the entire dithienylethene group to render the closed dication the most stable state and hence, allow for ring closure. The hexafluorocyclopentene ring however would be expected to be very poor in facilitating delocalisation of charge over both rings or facilitating rapid electron transfer between the thiophene moieties, resulting in ring opening to localize the charge on the thiophene rings. A further consideration is the role of substituents in the C5-position of the thienyl rings. The reversal of reactivity towards ring closure observed in **1Ho** (compared with **1Fo**) is achieved also by introduction of electroactive groups such as the methoxyphenyl unit **2F**.

It is well known that the solvent and nature of the electrolyte can have a pronounced influence on the reaction rates, in particular in systems exhibiting chemical reactions subsequent to electrochemical processes.[30] The solvent dependence on the electronic and redox chemistry of the **1H** was examined in detail to explore the role solvent and other environmental factors play in determining the chemical processes. Although the first oxidation process of both the **1Ho** and **1Hc** is predominantly solvent independent {**1Ho** – 1.12 (+/- 0.06) V, **1Hc** – 0.41 (+/- 0.07) V},[31] the separation between the first and second oxidation steps (ΔE) of the **1Hc** is very sensitive to both solvent and electrolyte. The relationship between ΔE, for the closed forms, and solvent acceptor number (AN), dielectric constant or polarity (ε) was explored, however no clear relationship was observed (Table 2.3).[32] In contrast a relatively good correlation ($R^2 = 0.92$) was observed between ΔE and the Guttmann solvent donor numbers (DN) (Figure 2.17), with ΔE found to decrease with increasing solvent donor strength (Table 2.3).[32] The relationship between solvent donor number and ΔE indicates that a significant degree of stabilisation of the monocation is achieved through solvation. As the solvent donor strength decreases the electron density on the closed form of the dithienylethene decreases for the monocation, which renders the second oxidation step more difficult and moves it to more anodic potentials. Furthermore, the effect of the solvent on the stability of the mono- and dication of the closed forms and the switching processes was examined for **1H**. In strong donor solvents neither process is reversible with the first oxidation step resulting in rapid decomposition. In weaker donor solvents, such as acetone, the first oxidation process of the closed form becomes fully reversible (*vide supra*). Nevertheless a pronounced scan rate dependence on the reversibility of the second redox process (with improved reversibility at higher scan rates) is observed in several weaker donor solvents with the formation of a stabilised cationic species being observed.

Table 2.3 Solvent dependence of electrochemical properties of **1Hc**.

Solvent[a]	ΔE (mV)	AN(solvent)	Dielectric constant (ε)	DN (solvent)
CH_3OH[d]	70	41.3	32.7	19
C_2H_5OH[d]	110	37.1	24.55	20
$(CH_3)_2SO$	115	19.3	46.68	29.8
DMF	160	16	36.71	26.6
THF	170	8.0	7.58	20
$(CH_3)_2CO$	190	12.5	20.70	17.0
CH_3CN	240	19.3	37.5	14.1
$CHCl_3$	200	23.1	4.81	<10
$PhNO_2$	305	14.8	34.82	4.4
CH_3NO_2	270	20.5	35.87	2.7
CH_2Cl_2	360	20.4	8.93	0
Diethylether[b]	490	3.9	4.3	19.2
THF[b]	320	8.0	7.58	20

[a]Unless stated otherwise, measured at 298 K, 0.1 M TBAP supporting electrode, scan rate 100 mV s^{-1}, [b]0.1 M NaBArF, [c]not measured [d] 0.1 M $NaClO_4$ supporting electrolyte. AN = acceptor number, DN = donor number, ΔE = separation first and second oxidation of ***1Hc.***

The value of ΔE obtained in diethyl ether solution is significantly higher than expected (*i.e.*, by comparison with THF, Table 2.3). This, initially surprising, result is due to the use of NaBArF (sodium tetrakis(3,5-di(trifluoromethyl)phenyl)borate) in place of Bu_4NPF_6 (TBAP) as supporting electrolyte.[33] Although, anions such as PF_6^- are generally accepted as being innocent with regard to their coordination properties, they are nevertheless stronger donor agents than the solvents themselves. The larger anion (*i.e.*, $BArF^-$) is a much weaker donor agent than more compact anions (*e.g.,* PF_6^-) and hence its ability to stabilise the monocation (**1Hc**$^+$) would be expected to be much less resulting in an increase in ΔE.[34] To test this, the effect of NaBArF in place of TBAP was examined in THF and indeed a striking dependence of ΔE on the electrolyte was observed {Δ(ΔE) % = 47 %}. Correction of the value obtained in diethyl ether[35] {ΔE = 490 mV} for the electrostatic contribution of the electrolyte results in a value {ΔE = 260 mV}, which is consistent for data obtained using TBAP. The increased values obtained using $BArF^-$ reflects its poorer donor properties compared with PF_6^-. The importance of the electrolyte is demonstrated further by the fact that in protic solvents (*i.e.*, MeOH and EtOH), values for ΔE lower than expected are obtained. Again the use of $NaClO_4$ as supporting electrolyte is a possible contributing factor to the lower value of ΔE. The effect appears to

be restricted to the anionic component of the electrolyte as in CH_3CN, KPF_6 instead of TBAP shows no observable effect on the oxidation chemistry.

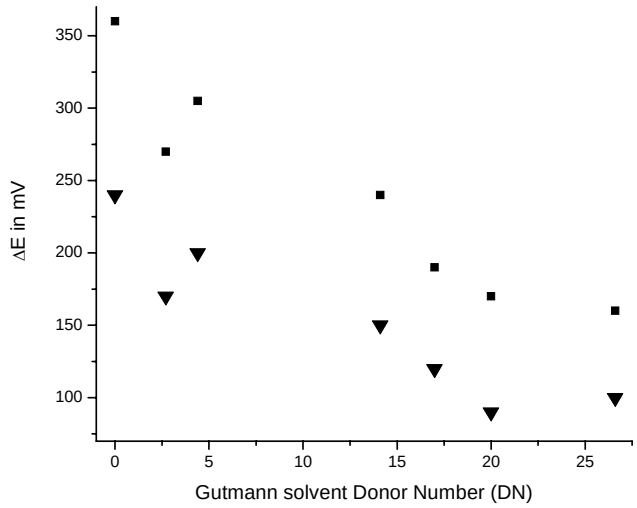

Figure 2.17 *Solvent dependence of ΔE for* ***5Hc*** *{$E_{½}$ (**5Hc**$^{+}$/**5Hc**$^{2+}$) - $E_{½}$(**5Hc**/**5Hc**$^{+}$)}, inverted triangles and* ***1Hc*** *{$E_{½}$ (**1Hc**$^{+}$/**1Hc**$^{2+}$) - $E_{½}$(**1Hc**/**1Hc**$^{+}$)} (squares) in 0.1 M TBAP/solvent at 0.1 V s^{-1}. In the case of MeOH and EtOH as a solvent 0.1 M $NaClO_4$ was employed as supporting electrolyte.*

During this research, cyclic voltammetry of **1Hc** and **1Ho** in diethyl ether showed a unexpected phenomenon. An irreversible oxidation process is observed at ca. 1.18 V (vs SCE), similar to the one observed for **1Ho** in acetonitrile. However, only negligible amounts of **1Hc**$^{2+}$ were observed on the return scan. Instead a reduction process at -0.1 V is observed, which is attributed to an additional species (**1Hx**). This new species is cationic and is formed by a reversible chemical rearrangement of **1Hc**$^{2+}$. The reduction process observed on the return cycle (at -0.1 V) is itself irreversible and results in two new oxidation processes being observed on the second scan at potentials coincident with those of **1Hc**. Similar behaviour was obtained for the closed form **1Hc**. Oxidation processes are observed at 0.345 V (**1Hc**$^{+}$) and 0.86 V (**1Hc**$^{2+}$) vs SCE. The first oxidation process is fully reversible, however, the second oxidation processes is irreversible and yields the reduction process at -0.1 V (as observed for **1Ho**) on the return cycle. Similar behaviour is observed in acetone, THF, DCM and $CHCl_3$, albeit with increasing reversibility of the second oxidation process of the closed form with increasing solvent donor strength.

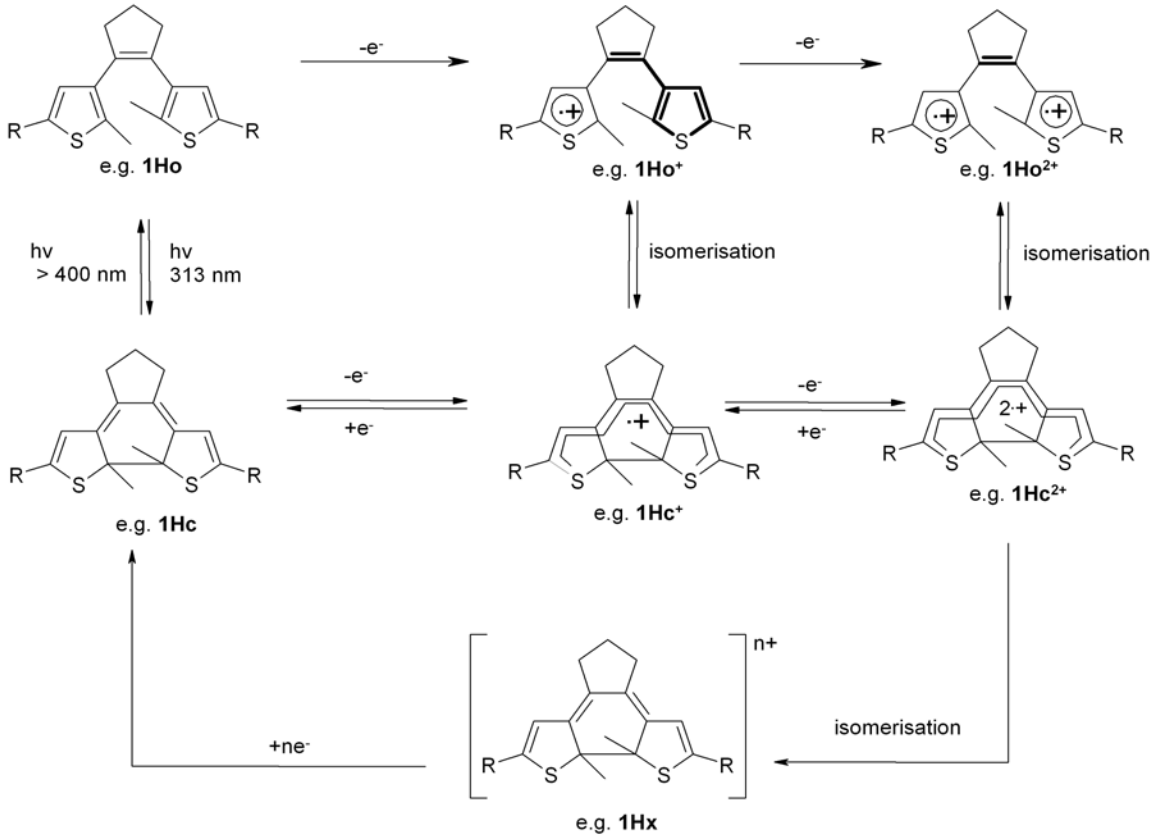

Figure 2.18 *General scheme for electrochemical processes observed in dithienylethene based systems. The observation of* ***1Hc***$^{+}$*, albeit at a low concentration, is significant and suggests ring closure occurs through the formation of* ***1Ho***$^{+}$ *leading to* ***1Hc***$^{+}$*, which is oxidised to* ***1Hc***$^{2+}$*. The structure of* ***1Hx*** *is arbitrary.*

This solvent dependence highlights the role of solvent in the stabilisation of **1Hc**$^{2+}$ as well as **1Hc**$^{+}$**.** In every case, at higher scan rates reversibility of the redox chemistry of **1Hc** is improved, confirming that the formation of **1Hx** is *via* an electrochemical-chemical (EC) mechanism and that the transformation is not directly coupled to the electron transfer process itself. It is clear that for **1Hc**, both the 1st and 2nd oxidation process is electrochemically reversible and that the formation of the oxidation product (**1Hx**, observed at -0.1 V) is due to a subsequent chemical reaction (presumably a reversible intramolecular reaction given its chemical reversibility) indicating an EC mechanism for the process. Hence overall, the conversion of **1Ho** to **1Hc** may be viewed as and ECEC mechanism in diethyl ether. A overview of the mechanisms discussed in this paragraph are presented in Figure 2.18. Theoretical calculations and ESR measurements on the charged compounds are under investigations at the moment.[36]

2.5 IR and Raman Spectroscopy

An essential prerequisite to the successful application of organic materials to memory devices is the achievement of non-destructive readout. In contrast to optical detection, infrared (IR) spectroscopy has proven to be useful in achieving non-destructive read-out,[37] as demonstrated with a recent example of a three bit eight states system.[38] Despite this recent progress in the application of vibrational spectroscopy as a non-destructive read-out method,[39] a general examination of the vibrational properties essential in tuning vibrational structure systematically is not yet available. In addition, the use of FTIR for practical applications is subject to technical limitations in portable devices. Raman spectroscopy offers an complimentary non-destructive readout approach to FTIR spectroscopy, due to its quite different technical requirements and its use of near-IR lasers and CCD detectors.[40] An extensive investigation of the IR and Raman vibrational structure of dithienylcyclopentene based switches was undertaken.[41] The effect of substitution of the perhydrocyclopentene unit for a perfluorocyclopentene unit and substitution at the C5-position of the thienyl rings on the both the IR and Raman spectra in the open and closed states was examined.

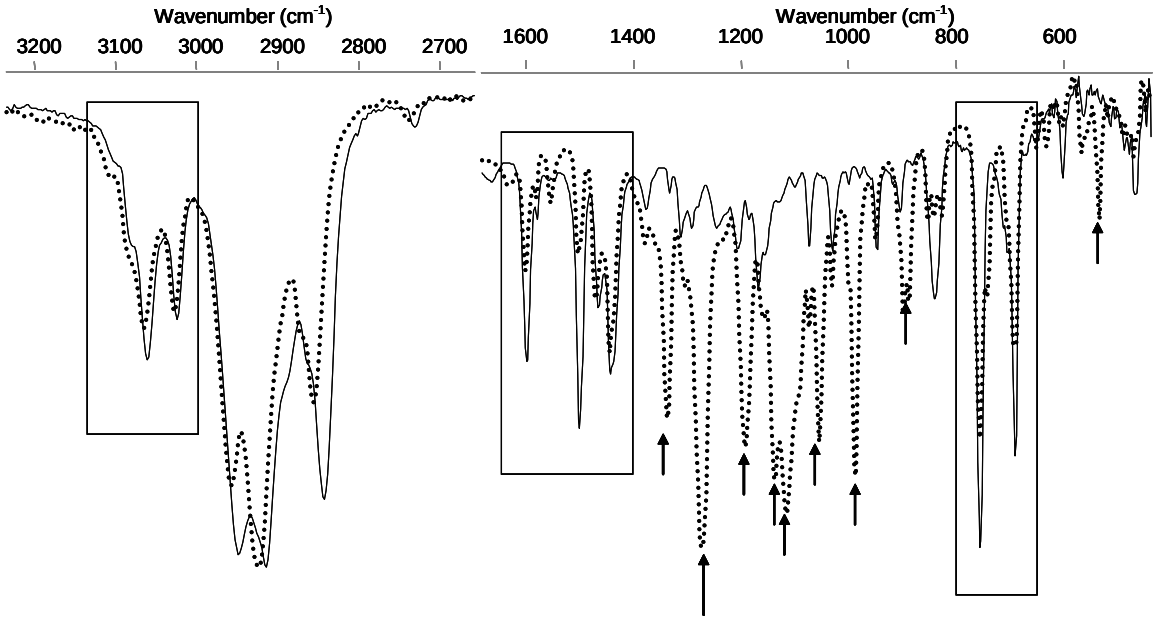

Figure 2.19 *Overlay of IR spectra of* ***1Ho*** *(solid line) and* ***1Fo*** *(dotted line), deposited from an acetonitrile solution onto KBr powder. The main vibrations arising from the perfluorocyclopentene ring are noted by black arrows. Boxes indicate from left to right aromatic C-H, aromatic C=C strech, and aromatic out of plane vibrations.*

The FTIR spectra of the **1H-11H** and **1F-3F, 9F** were recorded in the range 4000 to 500 cm^{-1}. The FTIR spectra of **1F-3F** for both the open and closed forms are in close agreement with spectra reported previously by Zerbi, Uchida and coworkers.[42] Comparison of the spectra of **1Ho-3Ho** with those of **1Fo-3Fo** (see Figure 2.19 for **1Ho** and **1Fo**) show the remarkably small influence of the cyclopentene unit on the vibrational structure of the core dithienylethene vibrations and the vibrations of the C5-substituents between 1450-1650 cm^{-1} (*vide infra*). The C-H stretching (2700-3200 cm^{-1}) is largely unaffected except for a decrease in aliphatic C-H vibrations of the cyclopentene unit at 2842 cm^{-1}. In the low wave number region (650-800 cm^{-1}) for the aromatic C5-substituted compounds (**1Ho-3Ho**, and **1Fo-3Fo**) the aromatic out of plane bending vibrations remain clear of interfering cyclopentene vibrations. The most dramatic difference in the spectra between the perhydro and perfluoro compounds is observed in the finger print region (800-1400 cm^{-1}). The very strong C-F vibrations serve to obscure the vibrations of the central dithienylethene core, rendering them unavailable for use in monitoring ring opening/closing reactions (*vide infra*).

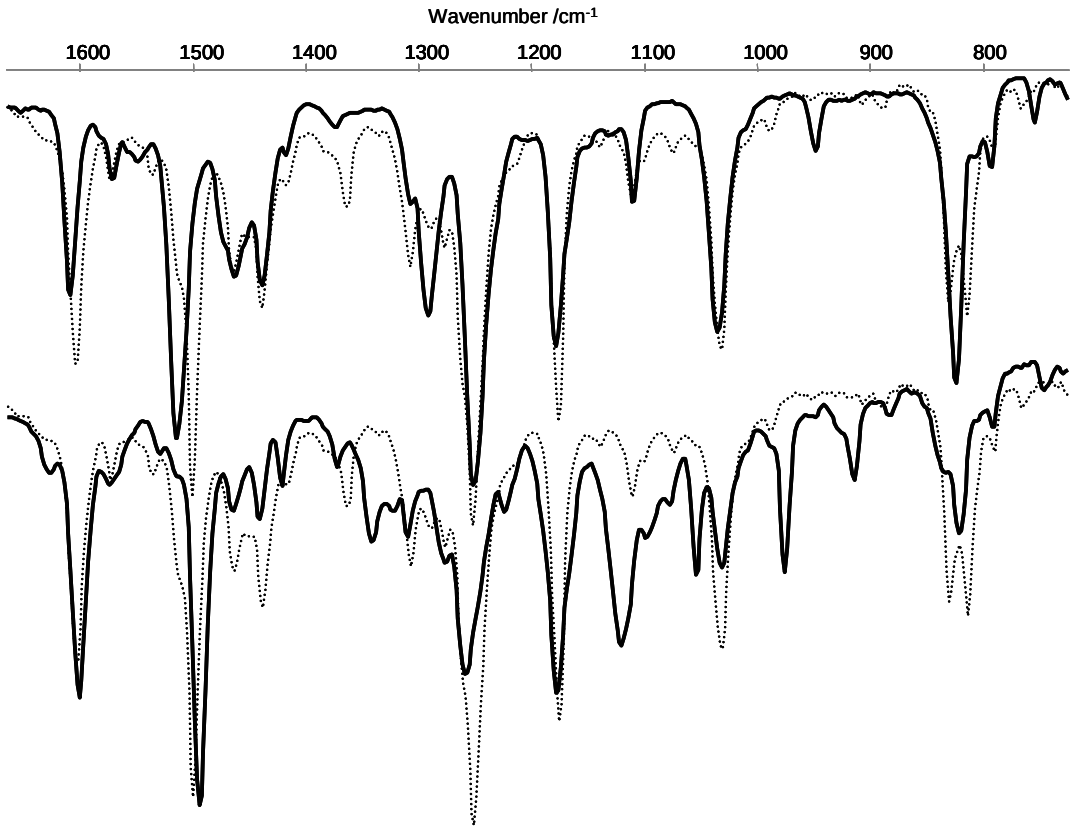

Figure 2.20 *Overlay of IR spectra of* ***2Hc*** *(dotted lines) overlaid with; upper set -* ***2Ho*** *(solid) and lower set -* ***2Fc*** *(solid) deposited from an acetonitrile solution onto KBr powder.*

Closed forms **1Hc-3Hc, 9Hc** and **1Fc-3Fc, 9Fc** could be prepared either on KBr directly or prior in solution from **1Ho-3Ho, 9Ho** and **1Fo-3Fo, 9Fo** by irradiation with UV light (λ = 313 nm). For **1-3F**, the spectra obtained match closely those reported in earlier studies, albeit with a higher degree of photoconversion in the present case. Comparison of the spectra of the open and closed state of the perhydrocyclopentene based switches (**1-11H**) reveals several similarities and differences (see Figure 2.20 for **3Hc/o** as a representative example). In the C-H stretching region (2700-3200 cm^{-1}) ring closure results in very minor changes to the bands,[43] however, in the 600-1600 cm^{-1} region large changes are observed, in particular in the aromatic out of plane bending bands (~820 cm^{-1}) and the ring breathing vibrations at ~1505 and 1605 cm^{-1}. The red-shift of the thienyl vibration at (1515 to 1500 cm^{-1}) reflects the formation of the extended *cis*-bis(*trans*-butadiene) system. The changes observed for the vibrational modes assigned to the peripheral aromatic rings (**1H-6H**), in particular the red-shift of the ring-breathing vibration at ca. 1600 cm^{-1}, indicates that a modest increase in electronic communication of the thiophene and phenyl ring systems upon ring closure. For **1Ho-11Ho** (1437, 1375, 1311, 1291, and 918 cm^{-1}) and **1Hc-11Hc** 1439, 1363, 1309, 1175, and 1140 cm^{-1} are characteristic, *e.g*. common bands.

It is clear that in the fingerprint region there are significant differences in the closed form for perhydro and perfluoro switches, which for example is shown in Figure 2.20 for **2Hc** and **2Fc**. Despite these difference in the fingerprint region, the overall spectrum is very similar as the most intense fibrations are present and almost overlapping for both compounds. It is interesting to note that significant changes between perhydro and perfluoro switches were observed by UV/Vis spectroscopy and electrochemistry, but apparently not for IR spectroscopy. The following signals are characteristic for **1Fc-3Fc, 9Fc** above 1000 cm^{-1}: 1626, 1440, 1373, 1341, 1225, 1187, 1120, 1077, 1032 cm^{-1} and for **1Fo-3Fo, 9Fo** 1337, 1194, 1137, 1111 cm^{-1}.

FTIR spectroscopy holds considerable potential towards non-destructive 'read-out', however, Raman spectroscopy, which can be viewed as a complimentary vibrational technique, offers an additional method for non-destructive readout. It is therefore surprising that, to date, only one example of the use of Raman spectroscopy for the investigation of dithienylethene switches has been reported.[39a] A key advantage for the use of Raman spectroscopy is the lower associated detector costs, as visible light rather than infrared light is used. However, the use of visible light may result in photoconversion occurring during the measurement, hence only excitation lines at wavelengths above the longest wavelength absorption of the closed form can be used. The solid state Raman spectra of the open forms of the dithienylethene switches were recorded by excitation at 785 nm (Figure 2.21-2.22). In contrast to IR spectroscopy the

effect of substitution of the perhydrocyclopentene unit for a perfluorocyclopentene has only a minor effect on the Raman spectrum (Figure 2.21) and although the effect of variation of substituents in the C5 position can be quite pronounced, the absorptions < 1100 cm^{-1}, the differences are largely confined to the relative band intensity (absorptions between 1700-1100 cm^{-1}), especially for the C5-phenyl substituted compounds (Figure 2.22).

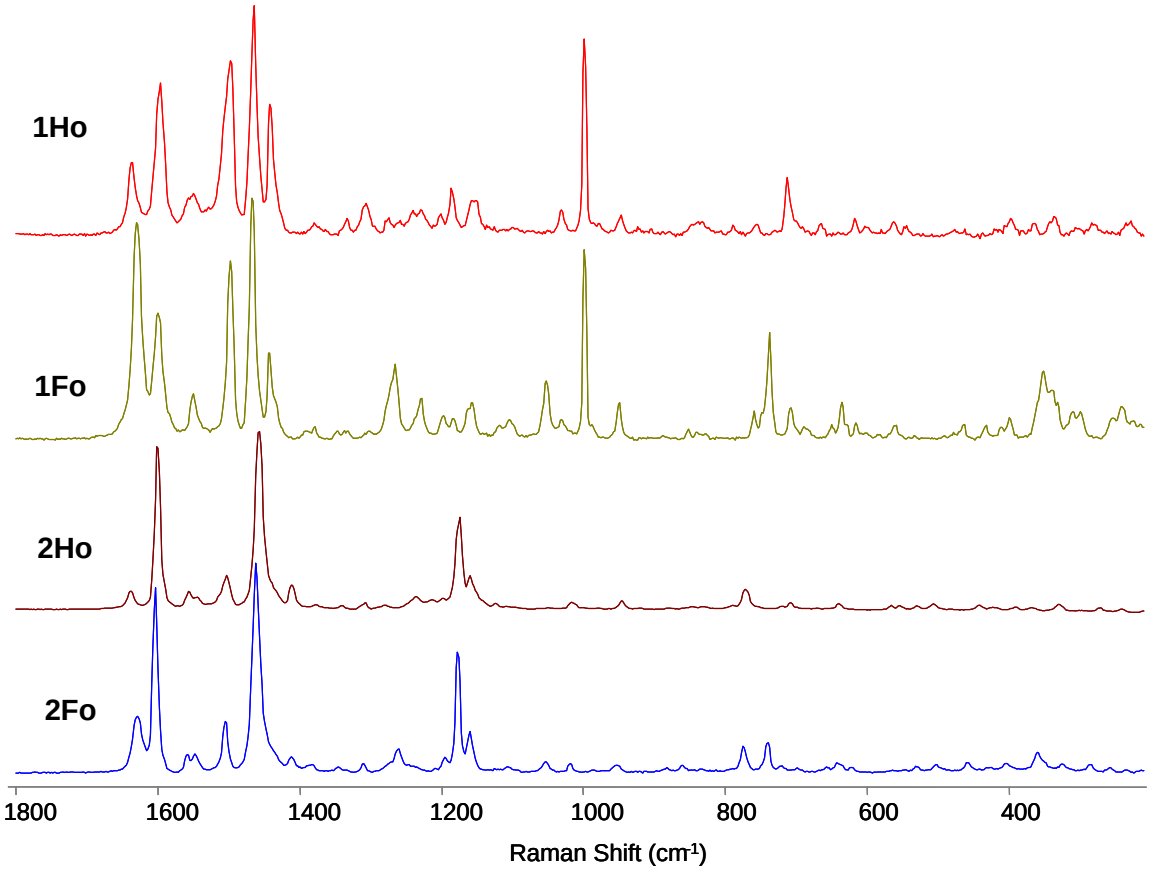

Figure 2.21 *Solid state Raman spectra of* ***1Ho***, ***1Fo***, ***2Ho*** *and* ***2Fo*** *(λ_{exc} = 785 nm).*

For all the dithienylethene switches examined no significant absorption of the closed form is observed at 785 nm (Table 2.1), making this wavelength suitable for non-destructive examination of the open and closed forms. The Raman spectra recorded at 785 nm excitation for **2Ho** and **2Hc** on KBr are presented in Figure 2.23. As for the IR spectra, ring closure of the open form results in a very dramatic change in the Raman spectrum. Whereas **2Ho** shows only very little Raman cross-section, for **2Hc** a huge increase in Raman cross-section is observed around 1500 cm^{-1} and between 1350-1150 cm^{-1}. It is therefore not only possible to monitor at a specific wavelength if the switch is in the closed or open state, as is also possible with IR spectroscopy, but just simple

integration of the signal intensity between 1800-700 cm^{-1} will indicate in which state the switch is.

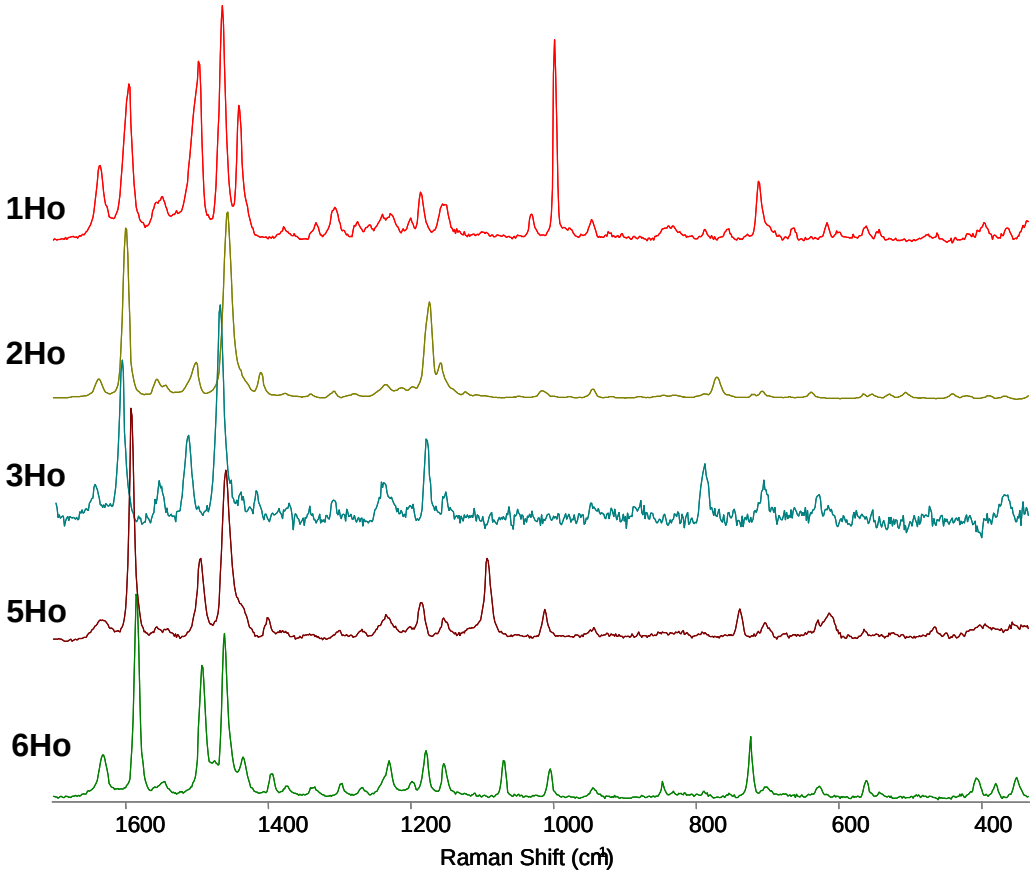

Figure 2.22 *Solid state Raman spectra of* ***1Ho-3Ho, 5Ho, 6Ho*** *(λ_{exc} = 785 nm). For the region > 1100 cm-1 the relative intensity changes while the position of the bands remains mostly the same. Below this region the substituent on the phenyl gives specific bands.*

In summary, IR changes for non-destructive readout can be observed not just for the C=C stretch absorptions as was reported in literature,[42c] but in the whole range between 600-1700 cm^{-1}. Perhydro and perfluoro switches show similar behaviour, however, the use of perhydro cyclopentene switches increases the range of the IR spectrum accessible to monitor the open/closed state due to the lack of strong C-F absorptions. Raman spectroscopy, in particular at preresonance wavelengths, shows considerable potential towards non-destructive readout. Large intensity differences between open and closed Raman spectra and the relatively simple spectra, combined with sensitivity of core vibrations to substitution facilitates global analysis procedures.

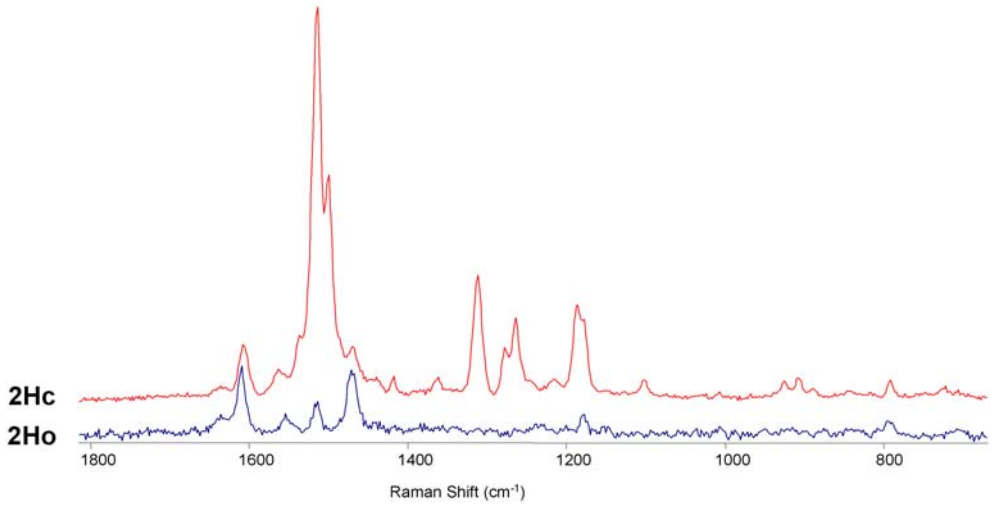

Figure 2.23 *Overlay of Raman spectra (λ_{exc} 785 nm, 6 * 20 s accumulations) of* ***2Ho*** *and* ***2Hc****. The band at 1636 cm^{-1} can be used as an internal reference, clearly showing the changes in total intensity between* ***2Hc*** *and* ***2Ho****.*

2.6 Other Research Areas for Switches

The borders between research areas are fading fast, not only within chemistry, but for the whole of science. Major effort is invested in combining different disciplines to achieve miniaturization in nanotechnology. Research on diaryl cyclopentene switches include various of host-guest complexations with switches and either crown ethers[44] or cyclodextrins.[45] Alternatively, they were used for inclusion in liquid crystalline materials,[46] whereas the magnetic properties have been explored by orientation of the dipole.[47] Ongoing research in our group is foccussed on fluorescence quenching upon switching from the open to the closed state, properties of polymers and molecular devices containing switches and optical switching in the crystalline state, which are shortly highlighted in this section.

Fluorescence Quenching

There is considerable interest in the development of efficient fluorescent molecules, which have the ability to turn fluorescence "on" or "off".[48] According to the literature, changes in fluorescence can be used in order to achieve nondestructive read-out, as described for IR spectroscopy (Chapter 2.5), when the excitation does not induce a ring opening- or ring closure reaction. This is, however, an intrinsic problem, because excitation will always be in the absorption region of the switch, and hence results in competition between ring opening or closing vs. fluorescence. Despite this problem,

fluorescence studies have been carried out in amorphous films,[49] on colloids,[50] and even on single molecules.[51] Several other systems have been reported,[52] for instance on fluorescence resonance energy transfer (FRET).[53] Hence it is interesting to explore the fluorescence properties of substituted perhydro dithienyl cyclopentene switches, since research in general on fluorescence properties of molecular switches is limited.[54] The highest reported quenching of fluorescence is in the order of 95% upon ring closure. Pyridine substituted switch **13H**[55] was reported previously, however no structural investigation into the fluorescence properties of perhydro switches have yet been reported. In ongoing research in our group our attention focusses on **14H-18H** which show fluorescence in the open form and reduced fluorescence in the closed form.[56] Whether this is related to for instance the reduction of the quantum yield for switching, a change in the equilibrium between photochemically active and inactive form, or something else is under investigation at this moment.

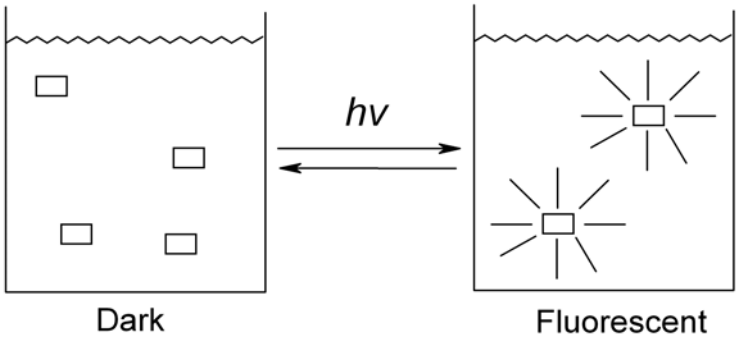

Figure 2.24 *Controling to turn fluorescence "on" or "off" by light is one of the areas where diarylethenes have been used.*

Molecular Switchable Devices

Current interests in materials includes responsive polymers that allow the construction of functional devices and materials. There have been several attempts to incorporate dithienyl cyclopentenes in either di- and oligomers[57] or polymers. These polymers fall into three different categories; coordination polymers[58] (in the crystalline state), or polymers with diarylethenes either in the backbone[59] or attached[60] to the polymer (Figure 2.25). Although incorporating the photochromic unit in the backbone will lead to high loading, it also often gives problems with conformational flexibility and rotational freedom, leading to low(er) PSS. Polymers containing diarylethenes have been made by reaction in polyurethane,[61] Wittig condensation,[62] radical polymerizations,[63] ring opening metathesis polymerization (ROMP)[64] and using Hay's method for oxidative polymerization.[65] Our research focusses on **11H** and **16H** and their corresponding

fluorinated counterparts in an attempt to use electrochemical polymerization to produce responsive polymeric materials. Although polymerization of **11H** and **16H** appears to occur readily, this project is still far from producing working responsive polymers.

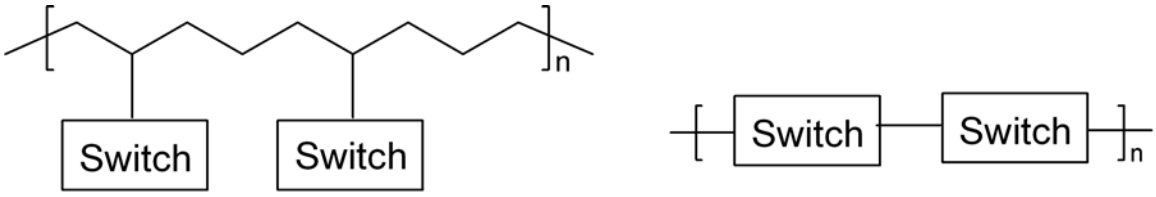

Figure 2.25 *Incorporation into polymers has been done either by attaching the switch to the backbone (left) or by incorporation in the backbone (right).*

Another field is molecular electronics, with single molecules being able to perform new operations that are currently inaccessible by conventional semiconductor technology.[66] Recently, we have demonstrated one-way optoelectronic switching of dithienylethenes on gold using break junction techniques (Figure 2.26).[67] Using this technique, nanometer size gaps between two gold electrodes can be prepared, which can accommodate a thiol functionalized switch. Using **12Hc** a resistance of 1MΩ was measured for the nanogap in the break junction, which increase to 1GΩ upon irradiation with visible light to **12Ho**. Unfortunally, subsequent irradiation with UV light did not result in a lowering of the resistance, indicating that ring closure does not occur, most likely due to quenching of the excited state. Future research using STM and gold nanoparticles (colloids) might lead to fully reversible, single molecule opto-electronics.

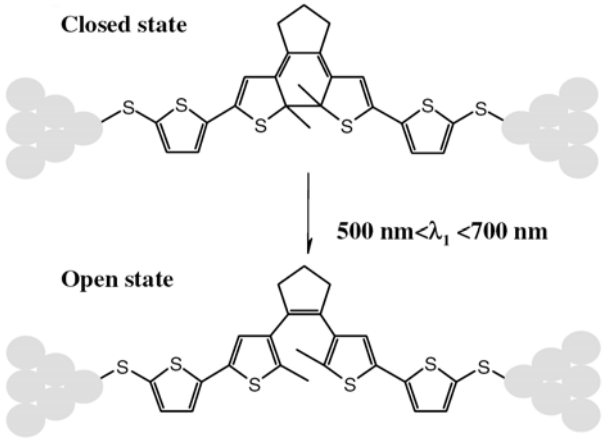

Figure 2.26 *The first molecular device with dithienyl cyclopenthene switches assembled between gold electrodes .*

The Crystal State

One of the main features of diaryl ethene switches is their ability to switch in the crystalline state. This phenomenon has attracted a lot of interest in the literature[68] and was reviewed in 2004 by Irie.[69] For most molecular switches the conformational changes needed are to large for the crystal lattice to accommodate, however this is not the case for diaryl ethene switches because the geometrical differences between open and closed form are small. An advantage of switching in the crystalline state is the improved quantum yield, because the open form is no longer subject to the dynamic equilibrium between active and inactive conformation. It has already been shown that perfluoro switches can be cycled more then 10^4 times without changing the shape of the crystal, and a range of different colors has been made (yellow, red, blue, and green).

Table 2.4 Crystallographic data for **7Ho**, **18Ho**, and **19Ho**.

Compound	**H6Cl**	**H6phBr-m**	**H6phphOC$_6$H$_{13}$**
Formula	$C_{15}H_{14}Cl_2S_2$	$C_{27}H_{22}Br_2S_2$	$C_{53}H_{60}O_2S_2$
fw (g mol^{-1})	329.31	570.41	793.19
crystal dim. (mm)	0.45 x 0.39 x 0.29	0.42 x 0.29 x 0.23	0.51 x 0.44 x 0.39
color	colorless	Light-blue	Colorless
habit	Block-shaped	Block-shaped	Irregular
crystal system	monoclinic	monoclinic	monoclinic
space group, no.	$P2_1/c$	$P2_1/c$	$C2/c$
a (Å)	8.7265 (7)	13.5963 (8)	18.076 (2)
b (Å)	12.311 (1)	11.8277 (7)	12.943 (1)
c (Å)	14.116 (1)	15.0520 (9)	19.832 (2)
V (Å^3)	1485.6 (2)	2336.3 (2)	4342.8 (7)
Z	1	4	4
ρ (g cm^{-3})	1.472	1.622	1.213
T (K)	100 (1)	100 (1)	100 (1)
μ (cm^{-1})	7.00	36.62	1.64
number of reflections	3654	5771	4559
# refined parameters	228	368	367
Fin. Agreement fact.:			
wR(F^2)	0.0753	0.0743	0.1210
R (F)	0.0284	0.0298	0.0451
GooF	1.043	1.027	1.037

For switching in the crystalline state, the distance between both reactive carbons should be less then 4.2 Å for ring closure to proceed. It is important to note that changing the solvent can have the effect that the switch is crystallizing in the photochemically inactive form. Switching phenomena for perhydro switches have not yet been reported in the

literature for the crystalline state. Perhydro switches are prone to precipitation instead of crystallisation, but after several attempts it was possible to obtain crystals suitable for X-ray analysis for **7Ho**, **18Ho**, and **19Ho** for which the crystallographic data are presented in Table 2.4 and Figures 2.27-2.29.[70] Crystals could also be obtained for **6Ho**, but the needles were to thin and X-ray analysis was not successful. Apparently, the addition of a halogen atom increases the crystallisation ability.

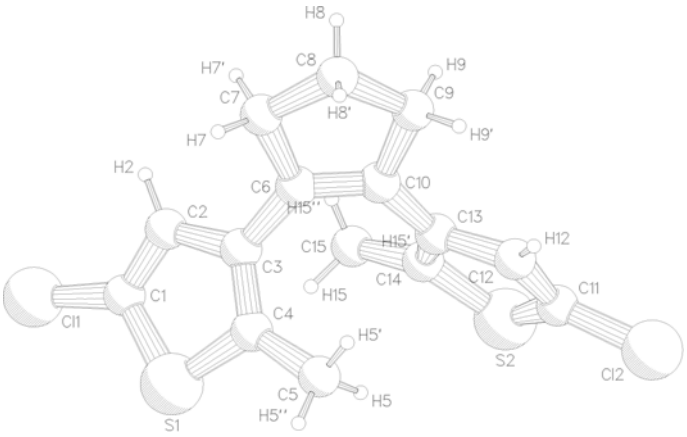

Figure 2.27 *X-ray structure of* ***7Ho****; the distance between C4 and C14 is 3.4894 (19) Å.*

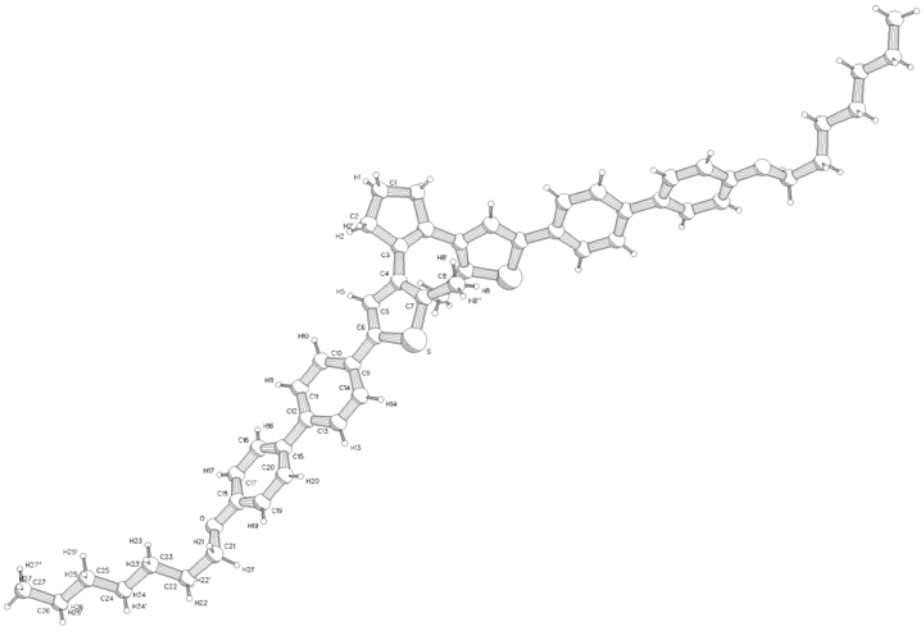

Figure 2.28 *X-ray structure of* ***18Ho****; the distance between C7 and C7' is 3.362 (2) Å.*

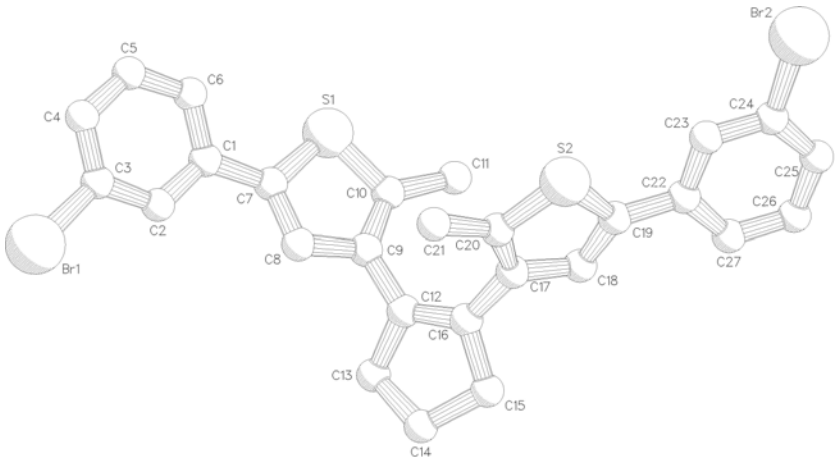

Figure 2.29 *X-ray structure of* ***19Ho****; the distance between C10 and C20 is 3.579 (3) Å.*

Colorless block-shaped crystals of **7Ho**, suitable for X-ray analysis, were obtained by recrystallisation from hexane. The distance between the reactive carbons C4 and C14 is well within the 4.2 Å (3.4894 Å) range and **7Ho** is oriented in the photochemical active conformation, so in principle switching should be possible in this crystal. However, no switching could be observed upon irradiation with UV light (λ = 313 nm), although switching was observed in solution previously (Table 2.1). The exact reason for the lack of switching is currently under investigation.

Colorless irregular crystals of **18Ho** were obtained from chloroform-d_1 and were suitable for X-ray analysis. The distance between the reactive carbons is only 3.362 Å and the molecule is in the photochemically active conformation, *i.e.* switching should be possible. Indeed, upon irradiation with λ = 313 nm a purple / blue color could be observed but upon breaking the crystal into smaller parts it was revealed that only the most outerlayer showed coloration, and not the whole crystal, as observed by optical microscopy. Therefore the smallest possible crystal suitable for X-ray analysis was irradiated in an attempt to color the whole crystal, but still only the most outer layer was colored. The absorption of the UV-light by the outer layer is apparently very efficient, which prevents the inner part from switching.

Light-blue block-shaped crystals of **19Ho** suitable for X-ray analysis were obtained by recrystallisation from n-hexane. The blue color of the crystal could indicates that after formation the crystal might have been accidently exposed to UV light, but the conversion is apparently so low that it was not detected by X-ray analysis. The molecule is in the photochemically active form and the distance of the reactive carbons is 3.579 Å, indicating that switching should occur, but again irradiation only lead to local conversion on the surface. Further irradiation with UV light of smaller pieces resulted in what under

an optical microscope looks like complete coloration of the crystal, but subsequent X-ray analysis still found the crystal in the open form. Aperently conversion to the closed form is low due to absorption of the UV-light by the outer layer of the crystal, although already higher then for **18H**. Currently investigations focus on improving and online monitoring of the photochemical conversion. Attempts to crystallise the closed form have been unsuccessful till now.

2.7 Conclusions

The synthesis for perhydro dithienyl cyclopentene switches is well established with a wide variety of functional groups that can be introduced. The addressability of the switches using UV and Vis light generally leads to high photoconversions, even though the absorptions in the UV region of the open and closed form overlap. Switching can also be accomplished electrochemically. The perhydro undergoes ring closure upon oxidation and the perfluoro compounds ring open upon oxidation. By introduction of electrochemically active groups the direction of switching can be inversed for perfluoro switches.

Although fluorescence can be use as a read-out, it is also destructive to the information stored because it uses the same absorption bands for excitation for switching from open to closed form. The use of either IR or Raman spectroscopy prevents this competitive process, and provides opportunities for non-destructive read-out. The use of perhydro instead of perfluoro derivatives open a much wider section of the IR spectrum for read-out due to the absence of strong C-F bond vibrations.

The first steps towards incorporation of these switches into molecular devices has been achieved. Not only is it possible to switch in the crystalline state, incorporation into polymers and even molecular electronics have great potential future prospect. In the following chapters these switches will be incorporated into low molecular weight organo gelators and their properties will be discussed.

2.8 Experimental

General Experimental

Starting materials were commercially available and were used without further purification. Melting points were determined on a Büchi melting point apparatus and are uncorrected. ^{1}H NMR were recorded on a Varian VXR-300 spectrometer (at 300 MHz) or a Varian 500 spectrometer (at 500 MHz) at ambient temperature. The splitting patterns

are designated as follows: s (singlet); d (doublet); dd (double doublet); t (triplet); q (quartet); m (multiplet) and br (broad). ^{13}C NMR were recorded on a Varian VXR-300 (at 75.4 MHz). Chemical shifts are denoted in δ (ppm) referenced to the residual protic solvent peaks. Coupling constants *J*, are denoted in Hz. Masses were recorded with a MS-Jeol mass spectrometer by A. Kiewiet, with ionisation according to CI^+, DEI or EI^+ procedures. Aldrich, silica gel, Merck grade 9385, (230-400 mesh) was used for column chromatography. The solvents were distilled and dried before use, if necessary, using standard methods. Reagents and starting materials were used as obtained from Aldrich, Acros Chimica or Fluka. For all spectroscopic measurements Uvasol (Merck) grade solvents or better were employed. Derivates synthesized are light sensitive and were therefore exclusively handled in the dark using brown glassware, and column chromatography was performed in yellow light. Irradiations were performed with a high pressure mercury/xenon lamp (200W, Oriel) or a xenon lamp (300W, Oriel) and the appropriate highpass or bandpass filters (Andover corporation). Additionally, UV light was obtained from a spectroline longlife filter at 313 and 365 nm.

Electrochemical Switching

The ferrocenium hexafluorophosphate was prepared by previously reported procedures. UV/Vis absorption spectra (accuracy ± 2 nm) were recorded on a Hewlett-Packard UV.Vis 8453 spectrometer. Electrochemical measurements were carried out on a Model 630B Electrochemical Workstation (CHInstruments). Analyte concentrations were typically 0.5 to 1 mM in anhydrous acetonitrile containing 0.1 M TBAP or 0.1 M $NaBArF^{71}$ (except where stated otherwise in the text). Unless otherwise stated a Teflon shrouded glassy carbon working electrode or 10 μm diameter platinum microelectrode (CHInstruments), a Pt wire auxiliary electrode and SCE or non-aqueous Ag/Ag^+ ion reference electrode were employed. Reference electrodes were calibrated using 0.1 mM solutions of ferrocene (0.38 V vs SCE in 0.1 M TBAP/CH_3CN). Solutions for reduction measurements were deoxygenated by purging with dry N_2 gas (presaturated with solvent) prior to the measurement. Cyclic voltammograms were obtained at sweep rates of between 10 mV s^{-1} to 50 V s^{-1}; differential pulse voltammetry (DPV) experiments were performed with a scan rate of 20 mV s^{-1}, a pulse height of 75 mV, and a duration of 40 ms. For reversible processes the half-wave potential values are reported; identical values are obtained from DPV and CV measurements. Redox potentials are +/- 10 mV. Spectro-electrochemistry was carried out using a custom made OTTLE setup comprising of a platinum gauze mesh working electrode (52 mesh, 0.1 mm wire diameter, Aldrich) a custom made 2 mm pathlength quartz cuvette (Chandos Intercontinental, UK) equipped with a solvent reservoir holding the reference electrode and a platinum gauze counter electrode (separated from the main solution by a ceramic frit) or in a SPECAC OTTLE

cell (0.5 mm pathlength). Measurements made at 0 ^{o}C were carried out using a Quantum Northwest Peltier cooled cell holder, modified for the UV.Vis spectrometer (*vide supra*).

UV/Vis Measurements

UV/Vis measurements were performed on a Hewlett-Packard HP 8453 diode array spectrophotometer. Stock solutions with Uvasol grade solvent or better were prepared by weighting out the diarylethene (typically 2.00 mg) on a five decimal balance and subsequently dissolution in 100.0 ml of solvent using brown glassware. These can be stored in the dark at r.t. without noticable change of the sample. Measurements were done in the dark in a 10 mm quartz cuvet (Hellma) with a stirring bar, a 'hagelslagje', in order to allow for in situ irradiation with either UV or Vis light. It should be noted that measuring does change the PSS slightly due to either ring opening or closing, but this effect can be minimized by stirring during the measurement.

Determination PSS

An NMR tube (diameter 5 mm) is charged with 1 mg of switch and 0.4 ml of the appropriate deuterated solvent on a Varian VXR-300 spectrometer (at 300 MHz). Differences in the ^{1}H NMR signals for either the thiophene C-H (around 7.0 ppm changes to 6.6 ppm) and / or the CH_2 next to double bond (around 2.8 ppm changes to 2.5 ppm) allowed the determination of the PSS. Depending on the light source used the switching is completed in 1-8 h. It should be noted that overexposure of the sample with UV light might cause degradation of the switch, which prohibits accurate determination of the PSS.

Fluorescence, IR, and Raman Spectroscopy

For fluorescence measurements, stock solutions made for UV/Vis were diluted 10 times or freshly made at 1 / 10 of the concentration used for UV/Vis. The fluorescence measurements were performed on a SPF-500C spectrofluorometer manufactured by SLM Aminco and a Fluorolog 3-22.

For IR measurements the diarylethene can either be grinded together with the KBr as a powder or added as a solution (usually acetonitrile) on the KBr, followed by evaporation of the solvent. Care has to be take that the sample layer is not too thick. Although ring opening using Vis light allows for thicker layers, ring closure is limited to the top layer due to an inner filter effect by the closed form. This will result in lower PSS, which can be avoided by filling out most of the sample container with KBr and depositing a small layer of KBr containing the switch on top of that. The IR spectroscopy measurements were performed on a Nicolet Nexus FT-IR apparatus.

For Raman measurements a Avalon R1-ST bench top Raman station with a 785 nm laser beam was used. The Raman scattering was collected and processed using Grams[AI]. All samples were measured as a powder.

X-ray diffraction: Crystal and Molecular Structure

Suitable light-blue-colored block-shaped crystals were obtained for **18Ho** by recrystallisation from hexane. A crystal with the dimensions of 0.42 x 0.29 x 0.23 mm was mounted on top of a glass fiber and aligned on a *Bruker*[72] *SMART APEX CCD* diffractometer (Platform with full three-circle goniometer). The diffractometer was equipped with a 4K *CCD* detector set 60.0 mm from the crystal. The crystal was cooled to 100(1) K using the *Bruker KRYOFLEX* low-temperature device. Intensity measurements were performed using graphite monochromated Mo-K$\bar{\alpha}$ radiation from a sealed ceramic diffraction tube (*SIEMENS*). Generator settings were 50 KV/ 40 mA. *SMART* was used for preliminary determination of the unit cell constants and data collection control. The intensities of reflections of a hemisphere were collected by a combination of 3 sets of exposures (frames). Each set had a different ϕ angle for the crystal and each exposure covered a range of 0.3° in ω. A total of 1800 frames were collected with an exposure time of 10.0 seconds per frame. The overall data collection time was 8.0 h. Data integration and global cell refinement was performed with the program *SAINT*. The final unit cell was obtained from the *xyz* centroids of 8485 reflections after integration. Intensity data were corrected for Lorentz and polarization effects, scale variation, for decay and absorption: a multi-scan absorption correction was applied, based on the intensities of symmetry-related reflections measured at different angular settings (*SADABS*)[73], and reduced to F_o^2. The program suite *SHELXTL* was used for space group determination (*XPREP*).[0]

The unit cell[74] was identified as monoclinic; reduced cell calculations did not indicate any higher metric lattice symmetry.[75] The space group $P2_1/c$, was derived from the systematic extinctions. Examination of the final atomic coordinates of the structure did not yield extra crystallographic or metric symmetry elements.[76,77] The structure was solved by Patterson methods and extension of the model was accomplished by direct methods applied to difference structure factors using the program *DIRDIF*.[78] The positional and anisotropic displacement parameters for the non-hydrogen atoms were refined. A subsequent difference Fourier synthesis resulted in the location of all the hydrogen atoms, which coordinates and isotropic displacement parameters were refined.

Final refinement on F^2 carried out by full-matrix least-squares techniques converged at $wR(F^2)$ = 0.0743 for 5771 reflections and $R(F)$ = 0.0298 for 4897 reflections with $F_o \geq$

4.0 $\sigma(F_o)$ and 368 parameters. The final difference Fourier map was essentially featureless: no significant peaks (0.60(8) e/Å^3) having chemical meaning above the general background were observed. The positional and anisotropic displacement parameters for the non-hydrogen atoms and isotropic displacement parameters for hydrogen atoms were refined on F^2 with full-matrix least-squares procedures minimizing the function $Q = \sum_h[w(|(F_o^2) - k(F_c^2)|)^2]$, where $w = 1/[\sigma^2(F_o^2) + (aP)^2 + bP]$, $P = [\max(F_o^2,0) + 2F_c^2] / 3$, F_0 and F_c are the observed and calculated structure factor amplitudes, respectively; ultimately the suggested a (=0.0409) and b (= 0.6297) were used in the final refinement. Neutral atom scattering factors and anomalous dispersion corrections were taken from *International Tables for Crystallography*.[79]

All refinement calculations and graphics were performed on a HP XW6200 (Intel XEON 3.2 Ghz) / Debian-Linux computer at the University of Groningen with the program packages *SHELXL*[80] (least-square refinements), a locally modified version of the program *PLUTO*[81] (preparation of illustrations) and *PLATON*[82] package (checking the final results for missed symmetry with the *MISSYM* option, solvent accessible voids with the *SOLV* option, calculation of geometric data and the *ORTEP* illustrations). Similar procedures were used for **19Ho** and **7Ho**.

General Procedure for the Suzuki-Reactions

Compounds **1-3**, **7-9**, **12H** and **1-3**, **7F** were prepared according to literature procedures developed by L.N. Lucas *et. al*.[12,14] For Suzuki reactions the boronic intermediate **A** is not isolated due to hydrolysis during workup.

1,2-Bis[5'-boronyl-2'-methylthien-3'-yl]cyclopentene (A):

Compound **7H** (70 mg, 0.2 mmol) was dissolved in anhydrous THF (8 ml) under a nitrogen atmosphere, and n-BuLi (0.31 ml of a 1.6 M solution in hexane, 0.5 mmol) was added using a syringe. This solution was stirred for 30 min at r.t., and B(*n*-OBu)$_3$ (0.18 ml, 0.6 mmol) was added. The resulting solution was stirred for 1 h at r.t. and used directly in the Suzuki cross coupling-reactions without any workup because boronic acid **A** is hydrolysed during isolation. Starting from **7F**, the lithiation is more convenient in diethyl ether, with less substitution occuring at the CF bonds.

1,2-Bis[5'-(4''thiomethoxyphenyl)-2'-methylthien-3'-yl]cyclopentene (4H):

To a solution of **7H** (250 mg, 0.76 mmol) in 10 ml THF under an inert atmosphere, *n*BuLi (1.4 ml, 1.6 M in hexane, 2.3 mmol) was added. After 1 h, B(OBu)$_3$ (0.60 ml, 2.3 mmol) was added to produce the bis-boronic ester intermediate. A separate flask was charged with 2-bromothioanisole (310 mg, 1.5 mmol), Pd(PPh$_3$)$_4$ (96 mg, 0.083 mmol), 5 ml THF, 4 ml 2 M $Na_2CO_{3(aq)}$ and ethylene glycol (5 drops). The mixture was heated to

80 °C and the preformed boronic ester in solution was added slowly from a syringe. The reaction mixture was refluxed for 3 h after which the reaction mixture was diluted with diethyl ether (50 ml) and washed with brine (50 ml). The brine solution was washed with an additional volume of ether (50 ml) and the combined organic phases were dried with Na_2SO_4 and concentrated. Chromatography over silica (hexane: CH_2Cl_2 10:1) gave a sticky compound which could be washed with hexane (excess) / CH_2Cl_2 (few drops) to yield **4H** (120 mg, 0.26 mmol, 35%). mp. 162-164 °C; ^{1}H NMR (300 MHz, $CDCl_3$): δ_H 1.97 (s, 6H), 2.06 (m, 2H), 2.47 (s, 6H), 2.82 (t, J = 7.2 Hz, 4H), 6.97 (s, 2H), 7.20 (d, J = 8.4 Hz, 4H), 7.38 (d, J = 8.4 Hz, 4H); ^{13}C NMR (75.4 MHz, $CDCl_3$): δ_C 14.4 (q), 16.0 (q), 23.0 (t), 38.4 (t), 123.7 (d), 125.6 (d), 127.0 (d), 131.5 (s) 134.2 (s), 134.6 (s), 136.6 (s), 137.0 (s), 139.1 (s); MS (EI): 504 [M^+]; HRMS calcd. for $C_{29}H_{28}S_4$ 504.108, found 504.108.

1,2-Bis[5'-(4''thioacetic acid phenyl)-2'-methylthien-3'-yl]cyclopentene (5H):
To a solution of **7H** (1.00 g, 3.05 mmol) in 40 ml THF under an inert atmosphere, *n*BuLi (6.0 ml, 1.6 M in hexane, 7.0 mmol) was added. After 1 h, $B(OBu)_3$ (2.50 ml, 6.5 mmol) was added to produce the bis-boronic ester intermediate **A**. A separate flask was charged with 1-bromo-4-(*t*-butylsulfanyl)-phenyl (1.00 mg, 6.2 mmol), $Pd(PPh_3)_4$ (400 mg, 0.083 mmol), 25 ml THF, 4 ml 2 M $Na_2CO_{3(aq)}$ and ethylene glycol (5 drops). The mixture was heated to 80 °C and the preformed boronic ester was added slowly via a syringe. The reaction mixture was refluxed for 3 h after which the reaction mixture was diluted with diethyl ether (50 ml) and washed with brine (50 ml). The brine solution was washed with an additional volume of ether (50 ml) and the combined organic phases were dried with Na_2SO_4 and concentrated. Chromatography over silica (hexane / ether 100:1) produced 1,2-bis[5'-(4''-*t*-butylsulfanyl-phenyl)-2'-methylthien-3'-yl]cyclopentene (800 mg, 1.35 mmol, 45%, 95% pure). ^{1}H NMR (300MHz, $CDCl_3$): δ_H 1.26-1.29 (m, 18H), 2.00 (s, 6H), 2.06 (m, 2H), 2.82 (t, J = 7.8 Hz, 4H), 7.03 (s, 2H), 7.24-7.49 (m, 8H). To a solution of this compound (500 mg, 0.80 mmol) and 0.40 ml acetylchloride in 10 ml CH_2Cl_2 under an inert atmosphere, BBr_3 (0.08 ml, 1.6 mmol) was added. The reaction mixture was stirred overnight after which the reaction mixture was diluted with diethyl ether (10 ml) and poured into 5 g ice-water. The phases were separated and the water layer was extracted with an additional volume of ether (20 ml) and the combined organic phases were dried with Na_2SO_4 and concentrated. Chromatography over silica (pentane/ether (500:1) yielded **5H** (130 mg, 0.23 mmol, 29%). mp. 61-64 °C; ^{1}H NMR (300 MHz, $CDCl_3$): δ_H 1.99 (s, 6H), 2.08 (m, 2H), 2.41 (s, 6H), 2.83 (t, J = 7.8 Hz, 4H), 7.06 (s, 2H), 7.35 (d, J = 8.1 Hz, 4H), 7.51 (d, J = 8.1 Hz, 4H); ^{13}C NMR (75.4 MHz, $CDCl_3$): δ_C 14.4 (q), 23.0 (t), 30.2 (q), 38.4 (t), 124.8 (d), 125.8 (d), 126.0 (s), 134.7 (s), 134.8 (d), 135.5

(s), 135.6 (s), 136.8 (s), 138.6 (s), 194.2 (s); MS (EI): 560 [M^+]; HRMS calcd. for $C_{31}H_{28}O_2S_4$ 560.097, found 560.097.

1,2-Bis[5'-(3''-bromophenyl)-2'-methylthien-3'-yl]cyclopentene (6H):
The same procedure was used as described for **4**, starting from **7** (1.00 g, 3.05 mmol), and n-BuLi (4.7 ml of 1.6 M solution in hexane, 7.59 mol), B(*n*-OBu)$_3$ (2.46 ml, 9.1 mmol), 1,3-dibromobenzene (3.40 g, 14.4 mol), Pd(PPh$_3$)$_4$ (0.41 g, 0.35 mmol), aqueous Na_2CO_3 (15 ml, 2 M) and 6 drops of ethylene glycol. Purification of the product by column chromatography (SiO_2, hexane) gave a white solid (504 mg, 29%). mp. > 124 °C (dec), ^{1}H NMR (300 MHz, $CDCl_3$) δ_H 1.97 (s, 6H), 2.07 (m, 2H), 2.82 (t, *J* = 7.2 Hz, 4H), 7.00 (s, 2H), 7.17 (t, *J* = 9.0 Hz, 2H), 7.33 (d, *J* = 7.5 Hz, 2H), 7.38 (d, *J* = 7.5 Hz, 2H), 7.62 (s, 2H); ^{13}C NMR ($CDCl_3$, 50.3 MHz) δ_C 14.4 (q), 23.0 (t), 38.4 (t), 122.9 (s), 123.9 (d), 124.8 (d), 128.2 (d), 129.7 (d), 130.3 (d), 134.7 (s), 135.4 (s), 136.5 (s), 136.8 (s), 137.9 (s); MS (EI): 570 [M^+], HRMS calcd for $C_{27}H_{22}Br_2S_2$ 571.949, found 571.951.

1,2-Bis[5'-carboxylic-acid-ethyl-ester-2'-methylthien-3'-yl]cyclopentene (10H):
To a solution of 75 mg of 1,2-bis[5'-carboxylic-acid-2'-methylthien-3'-yl]cyclopentene in 50 ml EtOH a catalytic amount of 30% HCl $_{(aq.)}$ was added. After stirring overnight, the solvent was removed to yield **10H** as a light-brown solid in quantitative yield. mp. 121-122 °C; ^{1}H NMR (300 MHz, $CDCl_3$): δ_H 1.32 (t, *J* = 6.9 Hz, 6H), 1.87 (s, 6H), 2.00-2.07 (m, 2H), 2.76 (t, *J* = 7.5 Hz, 4H), 4.28 (q, *J* = 6.9 Hz, 4H), 7.49 (s, 2H); ^{13}C NMR (75.4 MHz, $CDCl_3$): δ_C 14.3 (q), 14.8 (q), 22.8 (t), 38.6 (t), 61.0 (t), 129.6 (s), 134.2 (s), 134.7 (d), 136.5 (s), 142.5 (s), 162.1 (s); MS (EI): 404 [M^+]; HRMS calcd. for $C_{21}H_{24}O_4S_2$ 404.112, found 404.112.

1,2-Bis[5'-(thiophen-2-yl)-2'-methylthien-3'-yl]cyclopentene (11H):
The same procedure was used as described for **4**, starting from **7**. 2-Bromothiophene (0.04 ml, 0.4 mmol) was dissolved in THF (5 ml) and after addition of Pd(PPh$_3$)$_4$ (15 mg, 0.012 mmol), the solution was stirred for 15 min at r.t.. Aqueous Na_2CO_3 (1 ml, 2 M) and 6 drops of ethylene glycol were added, and the resulting two-phase system was heated in an oil bath till reflux. The solution of **A** was added dropwise with a syringe, after which the reaction mixture was refluxed for 2 h, and then allowed to cool to r.t. Diethyl ether (50 ml) and H_2O (50 ml) were added, and the organic layer was collected and dried (Na_2SO_4). After evaporation of the solvent the product was purified by column chromatography (SiO_2, hexane) to gave a purple solid (32 mg, 38%). mp. > 147 °C (dec.); ^{1}H NMR (300 MHz, $CDCl_3$): δ_H 1.94 (s, 6H), 2.04 (m, 2H), 2.79 (t, *J* = 12.5 Hz, 4H), 6.87 (s, 2H), 6.95 (t, *J* = 6.5 Hz, *J* = 3.3 Hz, 2H), 7.03 (d, *J* = 4.5 Hz, 2H), 7.13 (d, *J* = 8.5 Hz, 2H); ^{13}C NMR (75.4 MHz, $CDCl_3$): δ_C 14.3 (q), 22.9 (t), 38.5 (t), 122.9 (d),

123.7 (d), 124.5 (d), 127.6 (d), 133.0 (s), 134.0 (s), 134.5 (s), 136.3 (s), 137.7 (s); MS (EI): 424 [M^+]; HRMS calcd. for $C_{23}H_{20}S_4$ 424.045, found 424.042.

1,2-Bis(5'-(pyridin-4''-yl)-2'-methylthien-3'-yl)cyclopentene (13H):
The same procedure was used as described for **4**, starting from **7** (1.97g, 5.97 mmol), and n-BuLi (9.3 ml of 1.6 M solution in hexane, 14.88 mol), B(*n*-OBu)$_3$ (4.83 ml, 18 mmol), 4-bromopyridine.HCl (2.32 g, 0.12 mol), Pd(PPh$_3$)$_4$ (0.41 g, 0.35 mmol), aqueous Na_2CO_3 (15 ml, 2 M) and 6 drops of ethylene glycol. Purification of the product by column chromatography (SiO_2, methanol / CH_2Cl_2 1:20) gave a green solid (1.48 g, 60%). mp. > 124 °C (dec.), ^{1}H NMR (300 MHz, $CDCl_3$) δ_H 2.04 (s, 6H), 2.06-2.16 (m, 2H), 2.87 (t, *J* = 7.5 Hz, 4H), 7.19 (s, 2H), 7.36 (d, *J* = 5.4 Hz, 4H), 8.53 (d, *J* = 5.4 Hz, 4H); ^{13}C NMR (75.4 MHz, $CDCl_3$) δ_C 14.5 (q), 22.8 (t), 38.2 (t), 119.1 (d), 126.2 (d), 134.6 (s), 136.4 (s), 136.9 (s), 137.2 (s), 141.2 (s), 149.8 (d); MS (EI): 414 [M^+], HRMS calcd for $C_{25}H_{22}N_2S_2$ 414.122, found 414.121.

1,2-Bis(5'-[2-thienyl-5-(pyridin-4'-yl)]-2'-methylthien-3'-yl)cyclopentene (14H):
The same procedure was used as described for **4**, starting from **7** (70 mg, 0.2 mmol), and n-BuLi (0.31 ml of 1.6 M solution in hexane, 0.5 mmol), B(*n*-OBu)$_3$ (0.18 ml, 0.6 mmol), 2-bromothiophene-5-(pyridin-4'-yl) (0.064 g, 0.4 mmol), Pd(PPh$_3$)$_4$ (0.014 g, 0.12 mmol), aqueous Na_2CO_3 (1 ml, 2 M) and 6 drops of ethylene glycol. Purification of the product by column chromatography (SiO_2, hexane / ethyl acetate 1:2) gave a green solid (60 mg, 52 %). mp. > 157 °C (dec.), ^{1}H NMR (300 MHz, $CDCl_3$) δ_H 2.01 (s, 6H), 2.03-2.13(m, 2H), 2.83 (t, *J* = 7.5 Hz, 4H), 6.98 (s, 2H), 7.09 (d, *J* = 3.8 Hz, 2H), 7.46 (d, *J* = 3.8 Hz, 2H), 7.52 (d, *J* = 6.0 Hz, 4H), 8.55 (d, *J* = 5.4 Hz, 4H); ^{13}C NMR (75.4 MHz, $CDCl_3$) δ_C 14.4 (q), 33.5 (t), 38.4 (t), 119.3 (d), 123.9 (d), 125.2 (d), 126.1 (d), 132.4 (s), 134.7 (s), 136.0 (s), 136.5 (s), 138.7 (s), 139.6 (s), 141.1 (s), 150.2 (d); MS (DEI): 578 [M^+], HRMS calcd for $C_{33}H_{26}N_2S_4$ 578.098, found 578.095.

1,2-Bis(5'-[2,2'-bisthiophene-5-(pyridin-4'-yl)]-2'-methylthien-3'-yl)cyclopentene (15H):
The same procedure was used as described for **4**, starting from **7** (107 mg, 0.33 mmol), n-BuLi (0.52 ml of 1.6 M solution in hexane, 0.83 mmol), B(*n*-OBu)$_3$ (0.27 ml, 1 mmol), 5'-bromo-[2,2'-bisthiophene-5-(pyridin-4'-yl)] (0.21g, 0.66 mmol), Pd(PPh$_3$)$_4$ (0.023 g, 0.20 mmol), aqueous Na_2CO_3 (1 ml, 2 M) and 6 drops of ethylene glycol. Purification of the product by column chromatography (SiO_2, methanol / CH_2Cl_2 / Et_3N 1:20:1%) and subsequent trituration in CH_2Cl_2/ hexane gave a yellow solid (30 mg, 12 %). mp. > 210 °C (dec.), ^{1}H NMR (300 MHz, $CDCl_3$) δ_H 2.00 (s, 6H), 2.02-2.12 (m, 2H), 2.83 (t, *J* = 7.5 Hz, 4H), 6.92 (s, 2H), 7.00 (d, *J* = 3.6 Hz, 2H), 7.16 (d, *J* = 3.6 Hz, 2H), 7.19 (d, *J* = 4.1

Hz, 2H), 7.50 (d, *J* = 4.1 Hz, 2H), 7.57 (d, *J* = 6.0 Hz, 4H), 8.58 (d, *J* = 6.0 Hz, 4H); ^{13}C NMR (75.4 MHz, $CDCl_3$) δ_C 14.4 (q), 22.1 (t), 38.3 (t), 105.3 (d), 119.3 (d), 123.6 (d), 124.4 (s), 124.8 (d), 124.9 (d), 126.2 (d), 132.4 (s), 134.5 (s), 134.6 (s), 134.7 (s), 136.4 (s), 137.5 (s), 139.1 (s), 141.0 (s), 150.1 (d); MS (DEI): 742 [M^+].

1,2-Bis(5'-[2-thienyl-5-(thienyl-4'-yl)]-2'-methylthien-3'-yl)cyclopentene (16H):
The same procedure was used as described for **4**, starting from **7** (0.50 g, 1.49 mmol), and n-BuLi (2.5 ml of 1.6 M solution in hexane, 4.0 mol), B(*n*-OBu)$_3$ (1.2 ml, 4.6 mmol), 2-bromo-dithiophene (0.75 g, 3.1 mol), $Pd(PPh_3)_4$ (0.20 g, 0.18 mmol), aqueous Na_2CO_3 (15 ml, 2 M) and 6 drops of ethylene glycol. Purification of the product by column chromatography (SiO_2, pentane / DCM 16:1) gave a green solid (380 mg, 91%). mp. > 162 °C (dec)., ^{1}H NMR (300 MHz, $CDCl_3$) δ_H 1.96 (s, 6H), 2.06 (m, 2H), 2.81 (t, *J* = 7.5 Hz, 4H), 6.88 (s, 2H), 6.94 (d, *J* = 4.2 Hz, 2H), 6.99 (dd, *J* = 3.6 Hz, *J* = 0.15 Hz, 2H), 7.03 (d, *J* = 3.6 Hz, 2H), 7.13 (d, *J* = 3.6 Hz, 2H), 7.18 (d, *J* = 5.1 Hz, 2H); ^{13}C NMR (50.3 MHz, $CDCl_3$) δ_C 14.4 (q), 22.9 (t), 38.4 (t), 123.5 (d), 124.2 (d), 124.3 (d), 124.5 (d), 127.8 (d), 132.8 (s), 134.3 (s), 134.6 (s), 135.5 (s), 136.4 (s), 136.6 (s), 137.2 (s); MS (EI): 588 [M^+], HRMS calcd for $C_{31}H_{24}S_6$ 588.020, found 588.019.

1,2-Bis(5'-[2-thienyl-5-(phenyl-4'-yl)]-2'-methylthien-3'-yl)cyclopentene (17H):
The same procedure was used as described for **4**, starting from **7** (0.70 g, 2.14 mmol), and n-BuLi (3.5 ml of 1.6 M solution in hexane, 5.6 mol), B(*n*-OBu)$_3$ (1.72 ml, 0.64 mmol), 2-bromo-5-phenyl-thiophene (1.00 g, 0.4.2 mol), $Pd(PPh_3)_4$ (0.20 g, 0.18 mmol), aqueous Na_2CO_3 (15 ml, 2 M) and 6 drops of ethylene glycol. Purification of the product by column chromatography (SiO_2, pentane/diethyl-ether = 100/1) gave a green solid (180 mg, 15%). mp > 168 °C (dec.), ^{1}H NMR (300 MHz, $CDCl_3$) δ_H 1.97 (s, 6H), 2.05 (m, 2H), 2.82 (t, *J* = 7.5 Hz, 4H), 6.91 (s, 2H), 7.01 (d, *J* = 3.6 Hz, 2H), 7.17 (d, *J* = 3.6 Hz, 2H, 7.25 (d, *J* = 7.4 Hz, 2H), 7.35 (t, *J* = 4.5 Hz, 4H), 7.57 (d, *J* = 4.5 Hz, 4H); ^{13}C NMR (50.3 MHz, $CDCl_3$) δ_C 14.4 (q), 22.9 (t), 38.5 (t), 123.6 (d), 123.8 (d), 124.4 (d), 125.5 (d), 127.4 (d), 128.9 (d), 133.0 (s), 134.2 (s), 134.6 (s), 136.4 (s), 137.1 (s), 142.4 (s); MS (EI): 576 [M^+], HRMS calcd for $C_{35}H_{28}S_4$ 576.107, found 576.107.

1,2-Bis(5'-formyl-2'-methylthien-3'-yl)hexafluorocyclopentene (9F):
Under the same conditions as described for **9H**, n-butyllithium (1.6M in hexane, 0.13 ml, 1.8 mmol) was added to a stirred solution of **7F** (30 mg, 0.06 mmol) in anhydrous diethyl ether (5 ml) under nitrogen at r.t. for 30 min., after which the mixture was quenched with anhydrous N,N-dimethylformamide (0.05 ml, 0.6 mmol). Trituration from n-hexane / CH_2Cl_2 afforded the compound as a brown / orange solid (20 mg, 66%). mp. 182 °C; ^{1}H NMR (200 MHz, $CDCl_3$): δ_H 2.02 (s, 6H), 7.73 (s, 2H), 9.85 (s, 2H); ^{13}C NMR (50.3

MHz, $CDCl_3$): δ_C 15.2 (q), 110.1 (t), 115.7 (t), 125.8 (d), 135.3 (s), 136.5 (t), 142.2 (s), 151.3 (s), 181.5 (d); ^{19}F NMR (188.2 MHz, $CDCl_3$): δ_F -111.97 (t, J = 4.9 Hz, 4F), -133.55 (p, J = 4.9 Hz, 2F); MS (EI): 424 [M^+]; HRMS calcd. for $C_{17}H_{10}F_6O_2S_2$ 424.003, found 424.004.

References

[1] B.L. Feringa, Ed. *Molecular Switches* (Wiley VCH, Weinheim, **2001**).

[2] For an overview, see PhD thesis J.M. Kuipers; '*Azobenzene-substituted amphiphiles'*, **2005**, ISBN 90-367-2217-9.

[3] B.L. Feringa, R.A. van Delden, N. Koumura, E.M. Geertsema *Chem. Rev*. **2000**, 100, 1789-1816.

[4] W.F. Jager, J.C. de Jong, B. de Lange, N.P.M Huck, A. Meetsma, B.L. Feringa *Angew. Chem., Int. Ed.* **1995**, 34, 348.

[5] N. Koumura, R.W.J. Zijlstra, R.A. van Delden, N. Harada, B.L. Feringa *Nature* **1999**, 401, *6749*, 152-155.

[6] G. Berkovic, V. Krongauz, V. Weiss *Chem. Rev*. **2000**, 100, 1741-1753.

[7] Y. Yokoyama *Chem. Rev*. **2000**, 100, 1717-1739.

[8] (a) H.G. Heller, S. Oliver *J. Chem. Soc., Perkin Trans. 1* **1981**, 197-201. (b) P.J. Darcy, H.G. Heller, P.J. Strydom, J. Whittall, *J. Chem. Soc., Perkin Trans. 1* **1981**, 197-201.

[9] M. Irie, M. Mohri *J. Org. Chem*. **1988**, 53, *4*, 803-808.

[10] (a) *Memories and switches*, guest editor M. Irie *Chem. Rev.* **2000**, 100, 1683. (b) H. Tian, S.J. Yang *Chem. Soc. Rev*. **2004,** 33, *2*, 85-97.

[11] L.N. Lucas, J. van Esch, R.M. Kellogg, B.L. Feringa *Tetrahedron Lett.* **1999**, 40, 1775.

[12] L.N. Lucas, J. van Esch, R.M. Kellogg, B.L. Feringa *Chem. Commun*. **1998**, 2313.

[13] L.N. Lucas, J.J.D. de Jong, R.M. Kellogg, J.H. van Esch, B.L. Feringa *Eur. J. Org. Chem.* **2003**, 155-166.

[14] J.J.D. de Jong, L.N. Lucas, R.M. Kellogg, B.L. Feringa, J.H. van Esch *Eur. J. Org. Chem*. **2003**, 1887-1893.

[15] P.R. Hania, A. Pugzlys, L.N. Lucas, J.J.D. de Jong, B.L. Feringa, J.H. van Esch, H.T. Jonkman, K. Duppen *J. Phys. Chem. A* **2005**, 109, 9437-9442.

[16] M. Irie, K. Sakemura, M. Okinaka, K. Uchida *J. Org. Chem*. **1995**, 60, 8305-8309.

[17] (a) S. Irie, M. Irie *Bull, Chem. Soc. Jap*. **2002**, 75, *9*, 2071-2074. (b) S. Irie, M. Irie *Bull. Chem. Soc. Jpn*. **2000**, 73, *10*, 2385-2388. (c) S. Irie, T. Yamaguchi, H. Nakazumi, S. Kobatake, M. Irie *Bull. Chem. Soc. Jpn*. **1999**, 72, *5*, 1139-1142.

[18] (a) L. de Cola *Inorg Chem.* **2004**, 43, *9*, 2779-2792. (b) H. Port *J. Am. Chem. Soc.* **2000**, 122, 3037-3046. (c) T.J. Chow *Chem. Mater.* **2003**, 15, *23*, 4527-4532.

[19] (a) T. Iyoda, T. Saika, K. Honda, T. Shimidz *Tetrahedron Lett.* **1989**, 30, 5429-4432. (b) A. Fernandez-Acebes, J.-M. Lehn *Chem. Eur. J.* **1999**, 5, *11*, 3285-3292.

[20] (a) R.H. Mitchell, Z. Brkic, V.A. Sauro, D.J. Berg *J. Am. Chem. Soc.* **2003**, 125, 7581-7585. (b) S. Fraysse, C. Coudret, J.-P. Launey *Eur. J. Inorg. Chem.* **2000**, 1581-1590.

[21] (a) A. Peters, N.R. Branda *J. Am. Chem. Soc.* **2003**, 125, *12*, 3404-3405. (b) A. Peters, N.R. Branda *Chem. Commun.* **2003**, 4, 954-955. (c) B. Gorodetsky, H.D. Samachetty, R.L. Donkers, M.S. Workentin, N.R. Branda *Angew. Chem., Int. Ed.* **2004,** 43*, 21*, 2812-2815. (d) X.-H Zhou, F.-S. Peng Yuan, S.-Z. Pu, F.-Q. Zhao, C.-H. Tung *Chemistry Lett.* **2004**, 33, *8*, 1006-1007.

[22] In the present report, reversibility, quasi-reversibility and irreversibility refer to the chemical stability of the oxidised or reduced species. In all cases electrochemical reversibility ($E_{p,a}$-$E_{p,c}$ < 80 mV) is observed between 0.01 V s^{-1} and 2.0 V s^{-1} where the chemical stability of the oxidised / reduced species is sufficient to observe the return wave. Where the $I_{p,a}$ is not significantly different to $I_{p,c}$ peak the term reversible is applied, similarly quasi-reversibility refers to situations where chemical reversibility is scan rate dependent (*i.e*., observed only at higher scan rates).

[23] C. Hansch, A. Leo, R. W. Taft *Chem. Rev.* **1991**, 91, 165-195.

[24] Due to the limited data set available and the involvement of redox active substituents a similar correlation of the hexafluorocyclopentene based switches was not attempted.

[25] The two-electron transfer nature of the process is tentative and is difficult to confirm by standard experimental techniques.

[26] a) S. Encinas, L. Flamigni, F. Barigelletti, E. C. Constable, C. E. Housecroft, E. R. Scholfield, E. Figgmeier, D. Fenske, M. Neuburger, J. G. Vos, M. Zehnder *Chem. Eur. J.* **2002**, 8, 137-150. b) T. M. Pappenfus, K. R. Mann *Inorg. Chem.* **2001**, 40, 6301- 6307. c) A. Harriman, A. Mayeux, A. De Nicola, R. Ziessel *Phys. Chem. Chem. Phys.* **2002**, 4, 2229-2235.

[27] Electrochemical ring closure, albeit by reduction and oxidation of ancillary groups, has been observed previously by Lehn *et al*. and Branda *et al*.[21] for more complex systems.

[28] C. P. Andrieux, P. Hapiot, J. M. Saveant *Chem. Rev*. **1990**, 90, 723-738.

[29] At this moment it is unknown how the mechanism proceeds exactly. If a radical reaction takes place for ringclosure, it is possible to obtain the cis closed product, as was reported in reference 21c. Further research is underway to elucidate this phenomenon.

[30] F. Barriere, R. U. Kirss, W. E. Geiger *Organomet*. **2005**, 24, 48-52.

[31] The changes in $E_{½}$ (or E_{pa} in the case of irreversible process) is primarily assigned to the different contributions of the cell resistivity (iR drop) and junction potential due to the use of the SCE reference electrode. Similar variations in the $E_{½}$ of the ferrocene/ferrocenium redox couple were observed.

[32] V. Gutmann, G. Resch, W. Linert *Coord. Chem. Rev*. **1982**, 43, 133-164.

[33] A. Loupy, B. Tchoubar, D. Astruc *Chem. Rev.* **1992**, 92, 1141-1165.

[34] D. M. D'Alessandro, F. R. Keene *J. Chem. Soc., Dalton Trans*. **2004**, 3950-3954.

[35] This assumes that the contribution of the electrolyte is constant. This is incorrect as electrolytic activity is very dependent on solvent properties, however, given the similarities in the solvents being considered *i.e.*, THF and diethyl ether, in terms of DN, AN, ε, EnT, then the error in this assumption is expected to be small.

[36] M. Walko, J.J.D. de Jong, W.R. Browne, F. Hartl, J.J. McGarvey, J.H. van Esch, B.L. Feringa, *manuscript in preparation*.

[37] (a) K. Uchida, M. Saito, A. Murakami, S. Nakamura, M. Irie *Adv. Mater*. **2003**, 15, *2*, 121-125. (b) K. Uchida, M. Saito, A. Murakami, S. Nakamura, M. Irie *Chem. Phys. Chem*. **2003**, 4, 1124-1127.

[38] K. Uchida, M. Saito, A. Murakami, T. Kobayashi, S. Nakamura, M. Irie *Chem. Eur. J*. **2005**, 11, 534-542.

[39] (a) C. Okabe, T. Nakabayahi, N. Nishi, T. Fukaminato, T. Kawai, M. Irie, H. Sekiya *J. Phys. Chem. A* **2003**, 107, 5384-5390. (b) C. Okabe, N. Tanaka, T. Fukaminato, T. Kawai, M. Irie, Y. Nibu, H. Shimada, A. Goldberg, S. Nakamura, H. Sekiya *Chem. Phys. Lett.* **2002**, 357, 113-118. (c) D. Majumbar, H.M. Lee, J. Kim, B.J. Mhin *J. Chem. Phys*. **1999**, 111, 5866-5872.

[40] S.E.J. Bell *The Analyst,* **1996,** 121, 107R.

[41] J.J.D. de Jong, W.R. Browne, J.L. Barett, J.J. McGarvey, J.H. van Esch, B.L. Feringa, *manuscript in preparation*.

[42] (a) F. Stellacci, C. Bertarelli, F. Toscano, M.C. Gallazzi, G. Zerbi *Chem. Phys. Lett.* **1999**, 302, 563-570. (b) M. Saito, T. Miyata, A. Murakami, S. Nakamura, M. Irie, K. Uchida *Chem. Letters* **2004**, 33, *7*, 786-787. (c) A. Bianco, C. Bertarelli, J.F. Rabolt, G. Zerbi *Chem. Mater*. **2005**, 17, 869-874. The spectra reported previously described the range between 800 and 1650 cm^{-1} only; in the present report the spectral window is between 4000 and 550 cm^{-1}.

[43] The insensitivity of the CH stretching modes to ring closure is in agreement with ^{1}H NMR studies.

[44] M. Takeshita, M. Irie *Tet. Letters* **1998**, 39, 613. (b) M. Takeshita, M. Irie *J. Org. Chem*. **1998**, 63, 6643. (c) S.H. Kawai *Tet. Letters* **1998**, 39, 4445. (d) M. Takeshita, M. Irie *J. Chem. Soc., Chem. Commun*. **1996**, 1807.

[45] (a) A. Mulder, A. Jukovic, L.N. Lucas, J. van Esch, B.L. Feringa, J. Huskens, D.N. Reinhoudt *Chem. Commun*. **2002**, 22, 2734-3735. (b) A. Mulder, A. Jukovic, J. Huskens, D.N. Reinhoudt *Org. Biomol. Chem*. **2004**, 2, *12*, 1748-1755. (c) A. Mulder, A. Jukovic, W.F.B. van Leeuwen, H. Kooijman, A.L. Spek, J. Huskens, D.N. Reinhoudt *Chem. Eur. J.* **2004**, 10, *5*, 1114-1123.

[46] (a) T. Yamaguchi, T. Inagawa, H. Nakazumi, S. Irie, M. Irie *Chem. Mater.* **2000**, 12, *4*, 869-871. (b) K. Uchida, Y. Kawai, Y. Shimizu, V. Vill, M. Irie *Chemistry Lett.* **2000**, 6, 654-655.

[47] (a) K. Matsuda, M. Matsuo, M. Irie *J. Org. Chem*. **2001**, 66, *26*, 8799-8803. (b) F. Dietz, N. Tyutyulkov *Phys. Chem. Chem. Phys*. **2001**, 3, *20*, 4600-4605. (c) F. Dietz, N. Tyutyulkov *Chem. Phys*. **2001**, 265, *2*, 165-175.

[48] (a) A. Fernandez-Acebes, J.-M. Lehn *Chem. Eur. J.* **1999**, 5, *11*, 3285-3292. (b) J. Ern, A.T. Bens, H.-D. Martin, S. Mukamel, S. Tretiak, K. Tsyganenko, K. Kuldova, H.P. Trommsdorff, C. Kryschi *J. Phys. Chem. A* **2001**, 105, 1741.

[49] (a) T. Kawai, M.-S. Kim, T. Sasaki, M. Irie *Opt. Mater.* **2002**, 21, 275-278. (b) M. Kim, T. Kawai, M. Irie *Opt. Mater.* **2002**, 21, 271-274. (c) A. J. Myles, N. R. Branda *Macromol.* **2003**, 36, 298-303.

[50] K. Kasatani, S. Kambe, M. Irie *J. Polychem. Photobiol. A Chem.* **1999**, 11-15.

[51] (a) M. Irie, T. Fukaminato, T. Sasaki, N. Tamai, T. Kawai *Nature* **2002**, 420, 759-760. (b) T. Fukaminato, T. Sasaki, T. Kawai, N. Tamai, M. Irie *J. Am. Chem. Soc.* **2004**, 126, *45*, 14843-14849.

[52] (a) J.M. Endtner, F. Effenberger, A. Hartschuh, H. Port *J. Am. Chem. Soc*. **2000**, 122, 3037-3046. (b) T.B. Norsten, N. R. Branda *J. Am. Chem. Soc*. **2002**, 124, 7481. (c) T. Kawai, T. Sasaki, M. Irie *Chem. Commun.* **2001**, 711. (d) Q. Luo, X. Li, W. Zhu, H. Tian *Chemistry Lett.* **2003**, 32, *12*, 1116-1117. (e) Y.-C. Jeong, S.I. Yang, K.-H. Ahn, E. Kim *Chem Commun*. **2005**, 2503-2505.

[53] L. Giordano, T. M. Jovin, M. Irie, E. A. Jares-Erijman *J. Am. Chem. Soc*. **2002**, 124, 7481.

[54] (a) A. Osuka, D. Fujikana, H. Shinmori, S. Kobatake, M. Irie *J. Org. Chem*. **2001**, 66, 3913-3923. (b) K. Yagi, C. F. Soong, M. Irie *J. Org, Chem.* **2001**, 66, 5419-5423.

[55] (a) Fernandez-Acebes, J.-M. Lehn *Chem. Eur. J.* **1999**, 5, *11*, 3285-3292. (b) K. Matsuda, Y. Shinkai, M. Irie *Inorg. Chem*. **2004**, 43, *13*, 3774-3776.

[56] J.H. Hurenkamp, W.R. Browne, J.J.D. de Jong, L.N. Lucas, B.L. Feringa, J.H. van Esch *manuscript in preparation*.

[57] (a) H. Cho, E. Kim *Macro. Mol*. **2002**, 35, *23*, 8684-8687. (b) A. Peters, N.R. Branda *Adv. Mater. Opt. Elec*. **2000**, 10, *6*, 245-249.

[58] (a) B. Qin, R.X. Yao, H. Tian *Inorg. Chim. Acta* **2004**, 357, *11*, 3382-3384. (b) K. Matsuda, K. Takayama, M. Irie *Inorg. Chem*. **2004**, 43, *2*, 482-489. (c) K. Matsuda, Y. Shinkai, M. Irie *Inorg. Chem*. **2004**, 43, *13*, 3774-3776. (d) K. Matsuda, K. Takayama, M. Irie *Chem. Commun*. **2001**, 4, 363-364.

[59] (a) F. Stellacci, C. Bertarelli, F. Toscano, M.C. Gallazzi, G. Zotti, G. Zerbi *Adv. Mater*. **1999**, 11, *4*, 292-295. (b) E. Kim, S.Y. Cho *Mol. Crys. Liq. Cryst*. **2002**, 377, 385-390.

[60] E. Kim, Y.K. Choi, M.H. Lee *Macro. Mol*. **1999**, 32, *15*, 4855-4860.

[61] A.T. Bens, R. Comanici, B. Gabel, C. Kryschi, H.-D. Martin, H. Ritter *e-Polymers* **2003**, 3, 1-13

[62] (a) S. Wang, X. Li, B. Chen, Q. Luo, H. Tian *Macromol. Chem. Phys*. **2004**, 205, 1497-1507. (b) T. Kawai, T. Kunitake, M. Irie *Chemistry Lett.* **1999**, 9, 905-906.

[63] H. Tian, H.Y. Tu *Adv. Mater*. **2000**, 1597-1600.

[64] (a) A.J. Myles, Z.R. Zhang, G.J. Liu, N.R. Branda *Org. Letters* **2000**, 2, *18*, 2749-2751. (b) A.J. Myles, N.R. Branda *Macro. Mol*. **2003**, 36, *2*, 298-303. (c) T.J. Wigglesworth, N.R. Branda *Adv. Mater*. **2004**, 16, *2*, 123-125.

[65] (a) K. Uchida, A. Takata, M. Saito, A. Murakami, S. Nakamura, M. Irie *Adv. Func. Mater*. **2003**, 13, *10*, 755-762. (b) K. Uchida, A. Takata, S. Nakamura, M. Irie *Chemistry Lett.* **2002**, 4, 476-477.

[66] (a) A. Aviram, M. A. Ratner *Chem. Phys. Lett*. **1974**, 29, 277. (b) C. Joachim, J.K. Gimzewski, A. Aviram *Nature* **2000**, 408, 541. (c) J. C. Ellenbogen, J.C. Love *Architectures for Molecular Electronic Computers* (IEEE, New York, **2000**). (d) J. Park et al. *Nature* **2002**, 417, 722. (e) W. Liang, M.P. Shores, M. Bockrath, J.R. Long, H. Park *Nature* **2002**, 417, 725. (f) C. P. Collier, G. Mattersteig, E.W. Wong, Y. Luo, K. Beverly, J. Sampaio, F.M. Raymo, J.F. Stoddart, J.R. Heath *Science* **2000**, 289, 1172.

[67] (a) D. Dulic, S.J. van der Molen, T. Kudernac, H.T. Jonkman, J.J.D. de Jong, T.N. Bowden, J. van Esch, B.L. Feringa, B.J. van Wees *Phys. Rev. Lett.* **2003**, 91, *20*, Art. No. 207402. (b) T. Kudernac. J.J. de Jong, J. van Esch, B.L. Feringa, D. Dulic, S.J. van der Molen, B.J. van Wees *Mol. Cryst. Liq. Cryst*. **2005**, *430*, 205-210.

[68] (a) T. Yamada, S. Kobatake, K. Muto, M. Irie *J. Am. Chem. Soc*. **2000**, 122, *8*, 1589-1592. (b) S. Yamamoto, K. Matsuda, M. Irie *Angew. Chem*., *Int Ed.* **2003**, 42, *14*, 1636-1639. (c) M. Irie, T. Lifka, S. Kobatake, N. Kato *J. Am. Chem. Soc*. **2000**, 122, *20*, 4871-4876. (d) S. Kobatake, T. Yamada, M. Irie *Mol. Cryst. Liq. Cryst.* **2000**, 344, 185-190. (e) S. Kobatake, T. Yamada, K. Uchida, N. Kato, M. Irie *J. Am. Chem. Soc*. **1999**, 121, *11*, 2380-2386. (f) S. Irie, T. Yamaguchi, H. Nakazumi, S. Kobatake, M. Irie *Bull. Chem. Soc. Jpn*. **1999**, 72, *5*, 1139-1142. (g) S. Kobatake, M. Yamada, T. Yamada, M. Irie *J. Am. Chem. Soc*. **1999**, 121, *37*, 8450-8456. (h) M. Irie, K. Uchida *Bull. Chem. Soc. Jpn*. **1998**, 71, *5*, 985-996. (i) H. Miyasaka, T. Nobuto, A. Itaya, N. Tamai, M. Irie *Chem. Phys. Lett.* **1997**, 269, *3-4*, 281-285. (j) M. Irie, T. Lifka, K. Uchida *Mol. Cryst. Liq. Cryst. Sci. Tec. A* **1997**, 297, 81-84. (k) M. Irie, K. Uchida, T. Eriguchi, H. Tsukuki *Chem. Letters* **1995**, 10, 899-900. (l) S. Kobatake, S. Kuma, M. Irie *Bull. Chem. Soc. Jpn*. **2004**, 77, *5*, 945-951. (m) S. Kobatake, M. Irie *Chemistry Lett.* **2004**, 33, *7*, 904-905. (n) M. Morimoto, S. Kobatake, M. Irie *Chem. Rec*. **2004**, 4, *1*, 23-38. (o) T. Yamaguchi, Y. Fujita, H. Nakazumi, S. Kobatake, M. Irie *Tetrahedron* **2004**, 60, *44*, 9863-9869. (p) Y. Asano, A. Murakami, T. Kobayashi, S. Kobatake, M. Irie, S. Yabushita, S. Nakamura *J. Mol. Struc. Theochem*. **2003**, 625, 227-234. (q) S. Yamamoto, K. Matsuda, M. Irie *Org. Lett*. **2003**, 5, *10*, 1769-1772. (r) S. Yamamoto, K. Matsuda, M. Irie *Chem. Eur. J*. **2003**, 9, *20*, 4878-4886. (s) M. Morimoto, S. Kobatake, M. Irie *J. Am. Chem. Soc*. **2003**, 125, *36*, 11080-11087. (t) S. Kobatake, M. Morimoto, Y. Asano, A. Murakami, S. Nakamura, M. Irie *Chemistry Lett.* **2002**, 12, 1224-1225. (u) M. Morimoto, S. Kobatake, M. Irie *Chem. Eur. J*. **2003**, 9, *3*, 621-627.

[69] S. Kobatake, M. Irie *Bull. Chem. Soc. Jpn*. **2004**, 77, *2*, 195-210.

[70] Compound **19H** was prepared by Arjen Ellema.

[71] S.R. Bahr, P. Boudjouk *J. Org. Chem*. **1992**, *57*, *20*, 5545-5547.

[72] Bruker (**2000**). SMART, SAINT, SADABS, XPREP and SHELXTL/NT. Area Detector Control and Integration Software. Smart Apex Software Reference Manuals. Bruker Analytical X-ray Instruments. Inc., Madison, Wisconsin, USA.

[73] G.M. Sheldrick, *SADABS*, Version 2, *Multi-Scan Absorption Correction Program*, University of Göttingen, **2001**, Germany.

[74] A. J. M. Duisenberg *J. Appl. Cryst*. **1992**, 25, 92-96.

[75] A.L. Spek *J. Appl. Cryst*. **1988**, 21, 578-579.

[76] Y. Le Page *J. Appl. Cryst*. **1987**, 20, 264-269.

[77] Y. Le Page *J. Appl. Cryst*. **1988**, 21, 983-984.

[78] P.T. Beurskens, G. Beurskens, R. de Gelder, S. García-Granda, R.O. Gould, R. Israël, J.M.M. Smits, The *DIRDIF*-99 program system, Crystallography Laboratory, University of Nijmegen, **1999**, The Netherlands.

[79] *International Tables for Crystallography* Vol. C., Edited by A.J.C. Wilson, Kluwer Academic Publishers, Dordrecht, **1992**, The Netherlands.

[80] G.M. Sheldrick, *SHELXL-97*, *Program for the Refinement of Crystal Structures*, University of Göttingen, **1997**, Germany.

[81] A. Meetsma, *PLUTO, Molecular Graphics Program*, Version of February 2005, University of Groningen, **2005**, The Netherlands.

[82] A.L. Spek, *PLATON* **2004**, *Program for the Automated Analysis of Molecular Geometry* (*A Multipurpose Crystallographic Tool*), Version of March 2005, University of Utrecht, The Netherlands. A.L. Spek, *J. Appl. Cryst*. **2003**, 36, 7-13.